THE PENNSYLVANIA STATE UNIVERSITY
SCHREYER HONORS COLLEGE

DEPARTMENT OF ENGINEERING SCIENCE AND MECHANICS

PRELIMINARY EXPLORATION OF DIAMOND FORMATION AT ATMOSPHERIC
PRESSURE USING LASER SUSTAINED PLASMAS

ALAN GITHENS
Spring 2012

A thesis
submitted in partial fulfillment
of the requirements
for a baccalaureate degree
in Engineering Science
with honors in Engineering Science

Reviewed and approved* by the following:

Judith A. Todd
Department Head and P. B. Breneman Chair
Professor of Engineering Science and Mechanics
Thesis Supervisor

Clifford J. Lissenden
Professor of Engineering Science and Mechanics
Honors Adviser

Vladimir V. Semak
Associate Professor of Engineering Science and Mechanics and
Senior Research Associate

* Signatures are on file in the Schreyer Honors College and Engineering Science and
Mechanics office.

Abstract

An investigation of diamond chemical vapor deposition using laser sustained plasmas in open atmosphere was conducted. The main goal was to replicate past research, which successfully deposited a polycrystalline diamond film on a tungsten substrate. A cooling stage was developed to maintain the substrate surface temperature below 1000°C, ideal conditions for diamond formation. Scanning electron microscopy and Raman spectroscopy were used to study deposited films. Both graphite and polycrystalline diamond films were created. The Raman spectra of several locations on our samples matched the spectra of Bolshakov et al. (Bolshakov AP, Vostrikov VG, Dubrovskii VY, Konov VI, Kosyrev FK, Naumov VG, Ral'chenko VG. A laser plasmotron for chamberless deposition of diamond films. *Quantum Electronics*. 2005;35(4):385-389.), indicating that their work was replicated.

Table of Contents

Acknowledgements

List of Figures

1   Introduction

Diamond is an exceptional material due to its extremely high hardness, high thermal

conductivity, low coefficient of friction, and infrared transparency. Naturally occurring diamond,

however, is rare and expensive. To utilize the benefits of diamond while avoiding the high cost

of pure diamond crystals, many hard metals and metal composites such as titanium, steel, and

tungsten carbide-cobalt are coated with a polycrystalline diamond film. This film allows for a

much greater wear resistance and hardness than that exhibited by the bare metal.

The traditional method to create synthetic diamond films involves chemical vapor

deposition (CVD). In this process, a vacuum is drawn in a chamber around 10-100 torr. Next, a

hydrocarbon gas (methane being the most common) is heated inside the chamber to a high-

temperature plasma state at which the molecules ionize and create radicals suitable for diamond

deposition. A high concentration of hydrogen gas (a strong etchant) is also required in the

chamber. Hydrogen creates indentations in the substrate surface at which the carbon and

hydrocarbon radicals can nucleate and grow into either graphite or diamond structures [1].

The precursor gases, hydrogen and methane, are heated either by external sources (the

gases flow past hot filaments), plasmas, or combustion reactions. The most common hot-filament

and plasma assisted CVD methods require a vacuum for the precursor gases to break down into

the radicals necessary for diamond deposition.

These traditional CVD methods can create high quality, homogenous diamond films;

however, the deposition rates are low. Good quality films typically are grown at rates of 0.1 to 1

μm/hr [1].

Researchers have recently developed an alternative type of CVD using a high power

laser. In this technique, a jet of precursor gases is pumped coaxially out of the nozzle head of the

laser. The gas molecules can absorb energy from the laser beam and create a sustained plasma, or high energy optical discharge, at the nozzle head. This self-sustained plasma is referred to as a laser-sustained plasma (LSP) and stabilizes in atmospheric pressure.

The high energy of the gas molecules in the LSP combined with high ambient pressures (relative to traditional low pressure CVD techniques) could lead to unprecedented diamond deposition rates on the order of 10^3 to 10^4 μm/hr [2].

Initial experiments in this field, however, have yielded deposition rates of magnitude 10^1 to 10^2 μm/hr. Furthermore, the most common setup for this technique places the substrate directly under the path of the laser beam, i.e. the point of highest energy density. As a result, the substrate is not heated evenly. This causes problems with the homogeneity of the diamond films, as graphitic phases form if the temperature of the substrate is too high.

Further investigation in this field is required to optimize the technique. If good quality films at such high deposition rates can be attained (in atmospheric pressure nonetheless), the ease of creating diamond coatings would increase, and consequently, the cost would go down.

The design of this experimental technique requires the consideration of laser power, gas flow rate, precursor gas concentrations, the distance between plasma center (or the laser focal plane) and the substrate, substrate temperature, substrate material composition and preparation, atmospheric gas interactions, and experimental configuration. The presence of diamond/graphite species and diamond film quality can be determined using scanning electron microscopy (SEM) and Auger/Raman spectroscopy.

The objective of this thesis is first to replicate past LSP diamond CVD experiments to produce a polycrystalline diamond film. Then, using newly acquired information on the behavior of LSP-substrate interaction, develop a process to optimize diamond film growth rate and

quality. The main investigation will be focused on the experimental configuration—how to position the plasma and substrate relative to one another before and during the LSP exposure—to deposit an even, high quality, homogenous diamond film on a surface.

2   Literature Review

Diamond CVD by means of laser-sustained plasma is a relatively new area of interest. Much of the research thus far concerns the generation, maintenance, and stability of the plasma. This thesis, however, will concentrate on the actual diamond film created.

As mentioned in the introduction, diamond LSP CVD does not require a vacuum to operate, greatly reducing the complexity of setup. A widely adopted configuration for the technique developed by Varnin et al. [3] is shown in figure 1. The reactive gases were blown out
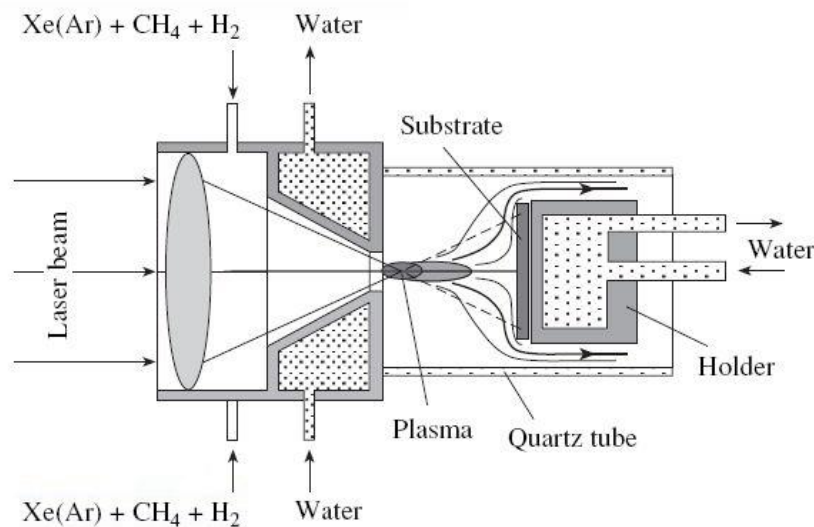
Figure 1. Standard experimental setup for diamond CVD using LSP [3].

of the laser head nozzle coaxial to the laser beam. The laser head was water cooled to prevent overheating/melting from the extremely hot plasma ball [3]. The LSP was initiated by focusing the laser beam at the throat of the nozzle onto the tip of a tungsten wire [4]. The tungsten atoms were vaporized and ionized into a highly energetic state and collided with the gas atoms blowing from the laser nozzle. These collisions knocked the electrons off of the gas atoms and, consequently, the gas atoms became ionized themselves. The end result was a plasma. When the rod was removed, the plasma remained intact because it absorbed the energy from the laser beam

(thus termed laser-*sustained* plasma).

The laser nozzle itself was aimed into a quartz tube chamber containing the substrate. The substrate was attached to a water cooled holder for temperature control, and this holder was separated from the quartz chamber walls by a very small clearance distance. The reactive gases were blown into the chamber and forced the atmospheric gases out by means of a slight overpressure, thus creating a controlled gas environment consisting of only the precursor reactive gases supplied. This controlled environment was necessary to keep out atmospheric gases, namely nitrogen, which can suppress the formation of diamond phase carbon [1, 5]. Bolshakov et al. presented an alternative method of controlling the environment that involved removing the quartz chamber altogether and using argon gas to shield the substrate from atmospheric nitrogen [5].

Several variations of this setup have been developed [2]. The substrate itself can be positioned to the side of the LSP, parallel to the laser beam as shown in figure 2 [2,5]. In this configuration, the laser beam did not hit the substrate directly, but the carbon radicals from the
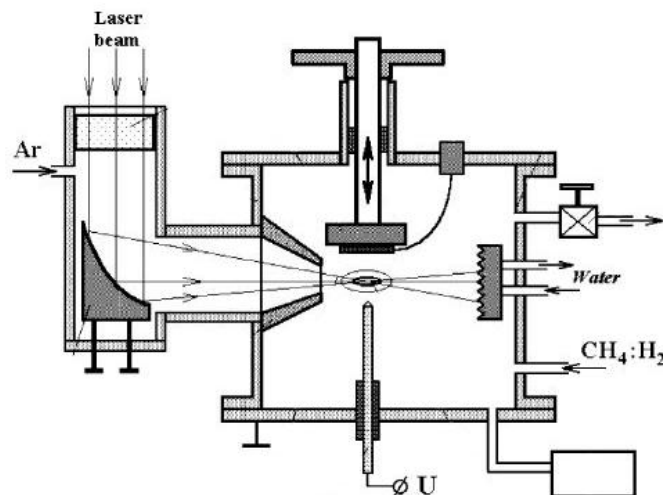
Figure 2. Experimental setup for diamond CVD by LSP with the substrate positioned parallel to the laser beam. Note that the beam never comes into contact with the substrate. Adapted from [2]

LSP were still able to contact the substrate to form diamond [2]. Another variation pumped the methane and hydrogen reactant gases directly into the main quartz chamber instead of through the laser nozzle. This allowed for a more stable LSP, but the convection currents from these gases have the possibility of extinguishing the plasma [5]. Bolshakov et al. placed the laser beam and gas jet pointing straight downward, angled the substrate 5°-10° relative to horizontal, and scanned the laser beam across the sample horizontally [5].

Less emphasis will be placed on specific parameter values used by past researchers. Laser type and mode geometry will likely differ depending on the laser, so this literature review will focus on general trends exhibited by others' previous experimentation and results.

The precursor gas must be composed mainly of xenon or argon for the LSP to form, as these inert gases have the lowest laser-induced discharge thresholds [3]. In other words, the plasma formed most readily when the precursor gases were purely noble. Introducing methane and hydrogen required a greater beam power for the LSP to remain stable. It has been found, however, that too high a power will extinguish the plasma [2]. The selection of beam power and reactive gas concentrations must be balanced—a greater concentration of methane and hydrogen will increase diamond formation rates but simultaneously demand more power for the LSP to remain stable.

The flow rate for the precursor gas mixture played a role in LSP maintenance, but not necessarily in diamond formation. It has been shown that both too low and too high a flow rate will not result in plasma formation. There is an optimum flow rate for the plasma maintenance laser threshold power. According to Bolshakov et al. [2], once the plasma was formed, flow rate did not otherwise significantly impact diamond deposition.

The selection of substrate material and surface pretreatment was crucial to the nucleation

of diamond and, consequently, deposition rates. Nearly all papers concerning diamond LSP CVD used molybdenum or tungsten for a substrate. These refractory metals withstood the high temperatures of the LSP, had low reactivity, and had relatively good thermal conductivities. Furthermore, it was shown that carbide forming substrates like Mo and W had greater nucleation rates and greater diamond adhesion compared to non-carbide forming materials [1].

Surface pretreatment was necessary in certain materials for any appreciable diamond nucleation to occur. These pretreatments included roughening, seeding, biasing, coating, ion implantation, irradiation, and carburization [1]. The requirement of these treatment techniques, however, is only understood for the more traditional CVD methods. Few of the current publications on diamond CVD by LSP experimented with different substrate pretreatment techniques. Bolshakov et al. [5] and Schwarz et al. [4] mechanically seeded the substrate with diamond particles less than one micron in size. Schwarz et al. used tungsten carbide-cobalt as a substrate, which required the removal of the cobalt matrix binder at the surface layer for diamond nucleation and growth. This can be accomplished using an acid etch [4].

While reported substrate temperatures varied considerably, it is clear that surface temperature is critical for diamond formation. Too high temperatures will result in graphite or other non-diamond carbon forms. Varnin et al. stated that deposition rates were most rapid when the substrate temperature was maintained at 1200°C, with diamond growth still possible as low as 600-700°C [3]. Bolshakov et al. [5], Metev [6], Konov et al. [7], and Schwartz et al. [4] witnessed the best diamond film between 800-1000°C, although the methods to monitor substrate temperature differed between groups. Some used an optical pyrometer to measure surface temperature [6] while others measured the temperature at the edge of the substrate using a thermocouple and approximated the overall surface temperature based on this reading [5, 7].

Diamond presence was detected using Raman spectroscopy. Raman spectroscopy is a characterization tool based on the inelastic scattering of monochromatic light (usually laser light) by a material. The laser light interacts with phonons in the lattice structure of a material and results in a shift in energy of the exiting laser light. The energy shift depends on the energy of the phonons and thus can give information about the vibrational modes in a system. Raman spectroscopy is most sensitive to symmetric covalent bonds with no natural dipole moment, such as those of the C-C bonds in carbon allotropes [8].

Every C-C bond in a pure carbon material vibrates with a certain frequency, and each band on the Raman spectrum corresponds to a specific vibrational frequency of these bonds. The most common bond frequencies are shown on the spectrum with the greatest intensity. The frequencies themselves are dependent on the bond strength, the orientation of the bond, and the weight of the atoms on each end of the bond in question. As such, Raman spectroscopy is an ideal tool to detect and characterize the differences of bonding in carbon allotropes [8].

For highly ordered carbon phases such as diamond crystals with near perfect sp3 bonding, the Raman spectrum consists of a sharp characteristic peak at 1335 cm^{-1}. Second order peaks appear on the spectrum due to two-phonon Raman scattering. Overtone and combination bands appear at 2184, 2468, and 2652 cm^{-1}, although their intensities are several orders of magnitude lower than the characteristic peak intensity [9].

Single crystal graphite with sp2 honeycomb structure has a characteristic peak at 1580 cm^{-1} [8]. Other carbon allotropes exhibit different spectra due to defects in the lattice structure as well as crystallite zone edge bonding disorder. Polycrystalline graphite exhibits a sharp peak at 1580 cm^{-1} (referred to as the G-line, or "graphite" line) which corresponds to the ordered sp2 bonding in the honeycomb monolayers of the material. A broad disordered carbon peak appears

at around 1360 cm^{-1} (referred to as the D-line, or "disordered" line). This peak corresponds to the first-order Raman scattering of zone edge phonons. Note that the characteristic peak of diamond is also referred to as the D-line, and the characteristic peak of single crystal graphite is called the G-line. The relationship and relative positions of the D- and G- lines gives information about the carbon bonds present [9]. For example, when the crystallites of polycrystalline graphite decreased in size, the Raman lines became broader and the G-line shifts to a slightly higher wave number. For highly disordered amorphous carbon, including diamond-like carbon, The D- and G- lines merged into a broad, asymmetric peak with a maximum intensity at 1500-1560 cm^{-1} [9].

TABLE IV. Raman spectra for various carbon compounds [A, asymmetric peak; B, broad peak (D and G lines are generally overlapped in the middle making a twin peak); S, sharp peak].

Materials	D line (cm^{-1})	G line (cm^{-1})	Reference
Natural diamond	(1332)$_S^a$		25,11
	(1336)$_S^a$		14
	(1334)$_S^a$		This work
Graphite			
Single crystal		(1580)$_S$	11,41
		(1585)$_S$	21
		(1584)$_S$	14
		(1575)$_S$	19
Small crystallite	(1360)$_B$	(1620)$_B$	23
Charcoal	(1360)$_B$	(1584)$_B$	11
Polycrystalline	(1355)$_B$	(1575)$_B$	19
Graphite	(1360)$_B$	(1580)$_B$	41
	(1354)$_B$	(1580)$_B$	This work
a-C, graphite			
e-Beam evap. or	(1360)$_B$	(1580)$_B$	41
Ar sputtered		(1550)$_A$	37
900 C annealed	(1350)$_B$	(1580)$_B$	9
	(1353)$_B$	(1598)$_B$	38
a-C:H, graphite			
Ar sputtered in H$_2$		(1580)$_A$	37
500 °C annealed	(1370)$_B$	(1590)$_B$	
a-C:H, DLC			
rf discharge in		(1520)$_A$	10
CH$_4$		(1357+1533)$_A$	This work
CVD diamond			
FACVD, CH$_4$/H$_2$	(1332)$_S^a$		13, 15, and this work
	(1333)$_S^a$		
	(1334)$_S^a$	(1355+1542)$_A$	
MPCVD, CH$_4$/H$_2$	(133)$_S^a$	(1550)$_A$	17
Flame, C$_2$H$_2$/O$_2$	(1334)$_S^a$+(1342)$_B$	(1576)$_B$	16

^{a}In general, D line designates a disorder peak, not the diamond peak.

Figure 3. Summary of the Raman spectra for various carbon phases [9].

Lee et al. summarized the expected Raman peaks for several carbon phases in figure 3 and also proposed a classification scheme for identifying carbon phases: Raman spectra showing a G-line greater than 1575 cm^{-1} indicated crystalline graphite, whereas a shift below 1575 cm^{-1} indicated amorphous carbon. Furthermore, graphite materials showed distinctly separate D- and G-lines whereas the D- and G- lines coalesced into a singular, asymmetric peak for amorphous phases [9].

The size of the diamond grains and general surface morphology was studied using scanning electron spectroscopy and atomic force spectroscopy. Diamond quality was also assessed using Auger spectroscopy [1]. To mimic the material properties of a pure diamond crystal, polycrystalline diamond films should have a low surface roughness [5].

Bolshakov et al. presented results on both the stationary LSP exposure setup described in figure 1 and the scanning tests described earlier [5]. Results from the stationary configuration revealed a key problem in the setup. The area where the laser beam hits the substrate overheated due to the high power density from the beam. As a result, the surface temperature was too high for diamond to form. An annular ring of diamond film formed around this centrally overheated site. The scanning tests were implemented to combat this overheating affect. Moving the substrate relative to the laser beam at a sufficiently high scanning rate was expected to reduce local overheating and provide a more uniformly heated substrate. Scanning also presented the possibility of depositing diamond coatings on a large area sample. The results for continuous scan speeds of 40 mm/s, however, still exhibited overheating and non-diamond growth on the path where the laser beam contacted the sample.

The configuration, shown in figure 2 proposed by Bolshakov et al. [5] appeared to be a promising method to avoid this overheating problem; the substrate did not come into contact

directly with the laser beam, when placed parallel with the laser. However, no results were published using this configuration.

The diamond films from Bolshakov et al. [5] were relatively rough, requiring post-production polishing to create the desired material properties. To reduce surface roughness, one can reduce the grain size of the diamond crystallites or control their orientation by aligning the (100) plane of BCC molybdenum or tungsten parallel to the film surface.

Konov et al. [7] observed an interesting phenomenon unique to the LSP-driven diamond CVD technique. The deposition temperature was much higher than for other CVD methods, and the maintenance of this temperature involved a carefully controlled cooling rate. When a graphite or black diamond film began to grow, the absorption on the surface changed such that the film absorbed more energy and caused a local increase in the substrate temperature. Since the formation of diamond is highly dependent on surface temperature, an increase in temperature can lead to graphitization and destruction of the overall film quality.

Deposition rates varied among the research groups. Metev et al. [6] reported the highest deposition rate on a molybdenum substrate of 120 μm/hr. His research group used lasers up to 12 kW in power. Bolshakov et al. [5] and Konov et al. [7] reported rates ranging from 2 to 50 μm/hr with a 3 kW laser system. Schwarz et al. [4] reported rates from 12 to 60 μm/hr using a laser system capable of 15 kW of power.

This literature review presents some promising evidence of high rate diamond CVD by LSP exposure. One key aspect of this thesis will be to replicate past experiments to see if diamond formation is possible with our 5 kW continuous wave CO_2 laser system. The ultimate goal of this research is to produce a homogenous, high quality diamond film across a non-localized surface area with high deposition rates relative to traditional diamond CVD techniques.

3   Experimental Procedures

3.1   Cooling Stage Design

As suggested in the literature review, substrate temperature was critical for diamond formation, and the sample surface was maintained in the range 800-1000°C. Due to the high energy yield of the laser beam and plasma, the substrate must be cooled. The easiest way to do this was to place the substrate on a water cooled stage.
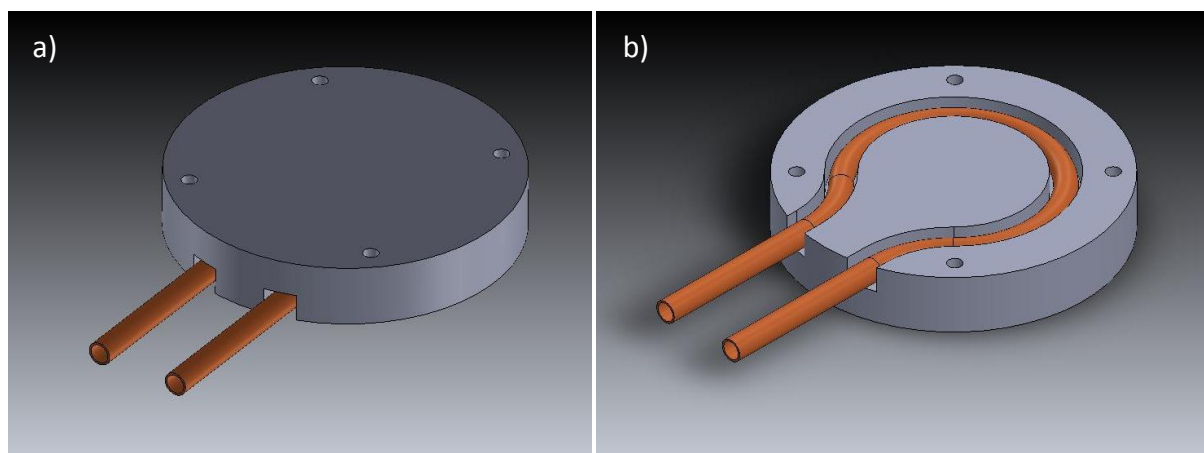
Figure 4. a) Top view of cooling stage design. b) Bottom view of cooling stage.

Most commercial cooling stages use copper or aluminum due to their high thermal conductivities, with melting temperatures of 1083°C and 660°C respectively. Because our experimental operating temperatures were expected to be above or close to these melting points, we needed to design our own high temperature cooling stage. The idea was similar to the commercial designs—to send cold water through a pipe which was inlayed in a block of metal. The only fundamental difference in our design was the material used. We compromised high thermal conductivity for high melting temperature because the stage would be rendered useless if it melted under the radiation of the beam and plasma. The stage was made of a stainless steel circular puck (melting temperature ~1400°C) with a milled groove around the center in which

rested a copper pipe. The copper pipe was held in place using silver solder. Figure 4a shows the top side of a SolidWorks rendering of our design on which the substrate sits. Figure 4b shows the underside. A schematic of the pipe can be found in Appendix A, and a schematic of the puck can be found in Appendix B.

On top of both the substrate and the stage was positioned a graphite shield, shown in figure 5a. There was a hole in middle of the shield through which the tungsten substrate was exposed to the laser beam and open atmosphere. The shield slightly overlaid the edges of the substrate and was clamped down, ensuring good contact between the cooling stage and substrate. A thin groove was made on the underside of the shield from one of the edges to the center, as can be seen in figure 5b. A thermocouple rested in the groove to monitor the temperature of the substrate.
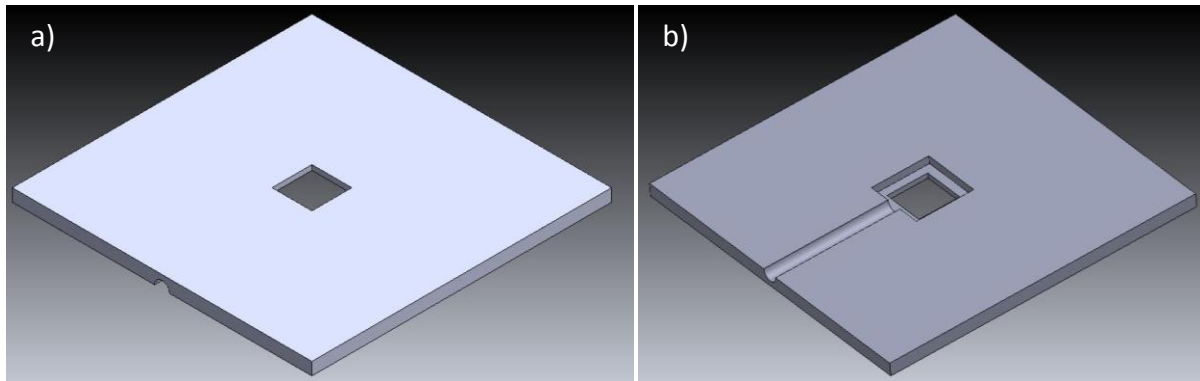
Figure 5. a) Top side of the cooling stage shield, made of graphite. b) Bottom side of cooling stage shield.

3.2   Experimental Configuration

Figure 6 shows the basic experimental configuration for our experiment. We used a 5 kW continuous wave CO_2 laser with a Q-mode Gaussian beam. The laser nozzle motion was controlled in the vertical z direction while the stage and substrate were controlled on moveable axes in the horizontal x and y directions. The laser beam was focused with a 5 inch focal length
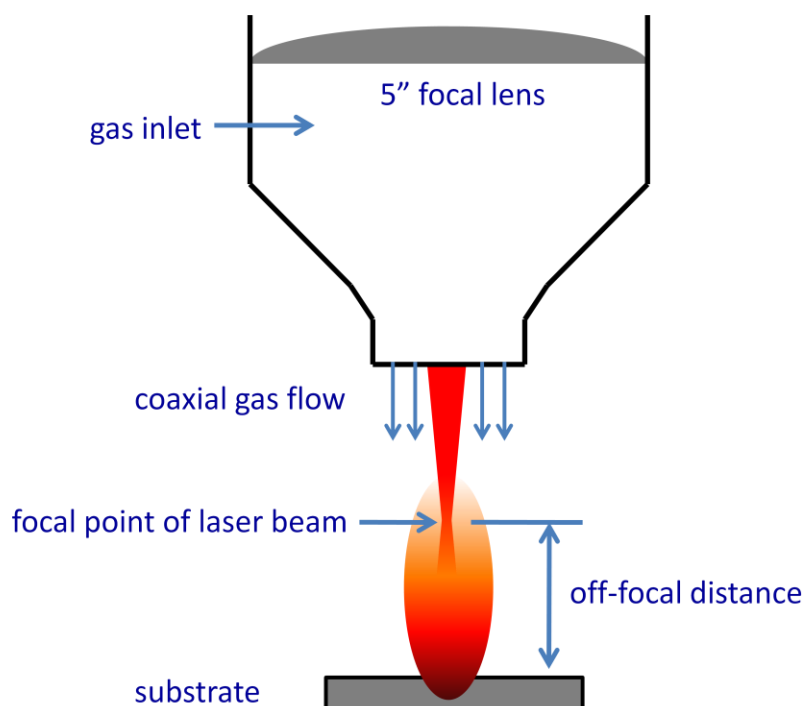
Figure 6. Experimental configuration for LSP exposure experiments.

lens and was aimed vertically downward toward the substrate. A precursor gas was pumped into the main laser nozzle chamber and flowed vertically downward, coaxial to the laser beam. The gas mixture used for diamond LSP CVD was 6.57% H_2, 2506 ppm CH_4, and the balance Ar. There was no gas containment system, so the experiment was completely open to the atmosphere. However, based on prior research conducted within our group, it was anticipated that a controlled containment/isolation system would not be needed, even though atmospheric nitrogen is known to prohibit diamond nucleation in traditional diamond CVD systems. Our

group has characterized and taken videos of the LSP with a high speed CCD camera and showed that when the LSP is appropriately positioned, the ionized species within the LSP and the shielding gas force most atmospheric gases away from the substrate surface. Laser induced plasma species, emitted from the substrate, may also force gases away from the surface.

In order to ignite the plasma, the focal point of the beam was scanned across a titanium plate. The high energy density of the laser beam vaporized the titanium atoms and ionized them. These highly energetic titanium species then collided with the incoming precursor gas (the methane mixture for diamond LSP CVD) and ionized these molecules. The effect continued and the plasma was sustained by a continuous supply of gas molecules and energy from the laser beam.

Figure 7 shows a photograph of our laboratory setup. The substrate sat on the cooling stage, with the water inlet and outlet connected to a chiller. The shield was clamped to the stage using machine screws.

The temperature of the sample was monitored with a K-type thermocouple. The junction bead was wedged between the substrate and graphite shield on the edge of the upper substrate surface so that the temperature was measured on the side of the substrate, not the area directly under the laser beam or the adjacent deposition zone. This was important to consider during testing because the actual surface temperature was higher in the center of the substrate than that displayed on the thermocouple meter. The thermocouple junction bead was initially spot-welded onto the substrate, but the high melting temperature of the tungsten prevented a secure bond from forming.

Figure 7. Laboratory setup of diamond LSP CVD system. Substrate temperature is controlled with a water cooled stage and monitored with a K-type thermocouple.

Several parameters were varied during the diamond LSP CVD process. These included 1) beam power—a greater laser power radiated more energy into the substrate and plasma, thus increasing the substrate temperature; 2) precursor gas flow rate—a higher gas flow rate increased convective heat transfer away from the substrate, thus reducing substrate heating.

Although the flow rate in the water cooled stage was adjustable, it was kept at a maximum to prevent overheating of the cooling liquid and flash boiling, which could damage the cooling stage and piping in the laser chamber.

Due to the design of the cooling stage and the constraints of the Swagelok hookups, the plasma-substrate orientation was limited to the standard configuration in figure 1. A re-design of the cooling stage may be needed for parallel orientation experiments as studied by Bolshakov et al. [2]. One important parameter in the configuration was the off-focal distance of the laser beam with respect to the substrate surface. Since the plasma core forms close to the focal point, decreasing the off-focal distance brings the LSP and substrate closer together. The reactive

species in the plasma collided with the surface more frequently, imparting their energy and thus increased the temperature of the substrate more rapidly. Furthermore, if the off-focal distance is too large (in an attempt to reduce overheating of the substrate), it is possible that the reactive species cannot reach the surface with enough frequency to produce any significant film. Past experimentation within our group showed that an off-focal distance of ~10 mm typically allowed for the plasma species to contact the surface and form a desired film.

3.3   Sample Preparation

Most researchers studying this deposition technique used tungsten and molybdenum due to their low reactivity and high melting temperatures. Swartz et al. [4] used tungsten carbide-cobalt in their experiments. This study investigated tungsten and tungsten carbide-cobalt.

3.3.1   Tungsten Carbide-Cobalt (WC-Co) Tool Material

WC-Co tool material is an extremely hard, wear-resistant metal matrix composite frequently used for tooling applications and drill bits. If diamond could be deposited on the surface easily, the wear resistance would improve and elongate the life of the hardware. This project investigated how a LSP reacted with the material.

For traditional diamond CVD, the tungsten carbide substrate needs to be etched beforehand to remove the cobalt binder from the surface, as cobalt has proven to inhibit diamond growth and causes adhesion problems between the film and substrate. Research conducted by Park et al. [10] investigated this phenomenon. They have shown that the cobalt binder moved to the film surface during deposition through diffusion and mass flow, encompassing diamond nucleation sites and prohibiting their growth.

It is possible that the diamond LSP CVD technique may circumvent this issue in several ways. The first hypothesis was that the energy of the plasma would melt or vaporize the cobalt locally from the surface, leaving only the tungsten carbide particles behind (due to their much higher melting point). The plasma could effectively etch the surface. Another hypothesis was that because deposition rates are significantly greater than in traditional CVD techniques, diamond could nucleate and grow before the cobalt binder diffuses to the surface.

To test our theory, we inserted a tungsten carbide rod (1.6 mm diameter) into a pure argon LSP 1 mm away from the focal point of the laser beam for 5 seconds. Figure 8 shows the experimental setup. Laser power was 2.5 kW and gas flow rate was 10 L/min. Note the WC rod was not placed on the water cooled stage in this experiment.
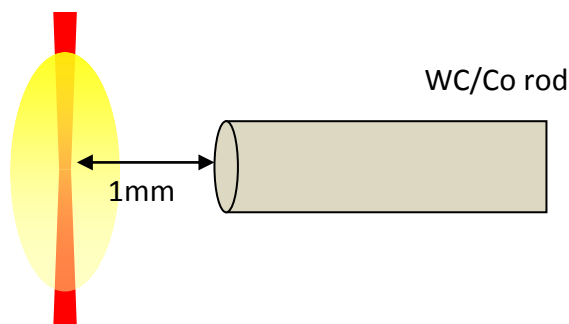
Figure 8. Diagram of a tungsten carbide/cobalt rod inserted into an Ar LSP 1 mm from the center of the laser beam.

We examined the longitudinal cross section of the rod after LSP exposure using optical microscopy and scanning electron microscopy (the circular cross section was not investigated). The rod was mounted in a Bakelite puck and ground down 0.4 mm using SiC grit paper. A vacuum impregnation technique was then applied to fill the pores with epoxy to help prevent pull-out. The sample was ground down an additional 0.2 mm before polishing. A polish was attained using a series of decreasing diamond particle size suspensions, followed by a final polish with colloidal silica particle < 1 μm. The goal was to determine whether there were any

signs of etching along the outer surface of the rod, and if so, how these effects changed with respect to distance from the plasma core.

During sample preparation, the tip of the rod closest to the plasma broke off easily, suggesting it turned brittle and weak during the experiment. This was unexpected since tungsten carbide-cobalt exhibits an extremely high hardness, but it could be a sign of successful cobalt metal binder removal.

Figure 9 shows an optical micrograph of the cross section. Craters or bubbles were observed throughout the LSP affected region. These pores might have been created by carbon dioxide bubbles forming in the metal matrix under the following reaction: $WC + O_2 \rightarrow W + CO_2$. The overall diameter of the rod also increased in the middle of the photographed view. The craters slowly tapered off away from the center of the LSP and, at a certain point away, stopped altogether.
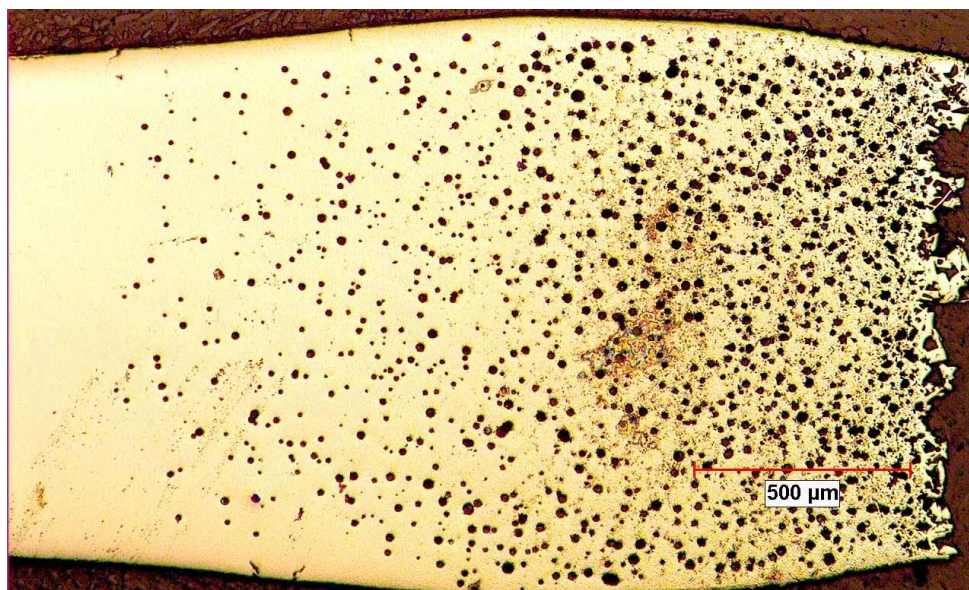

Figure 9. Longitudinal cross section of tungsten carbide rod. LSP core was closest to the right side during exposure.

Figure 10 shows a higher magnification of the tip where part of the sample broke off. The tungsten carbide particles appeared as geometric shapes in the cobalt binder. It was evident that

the WC grains experienced significant grain growth due to the high energy of the LSP. This likely explained why the tip became so brittle. The cobalt binder (removed by vaporization or melting) no longer enveloped the large grains, and thus any slight impact would cause fracture along the grain boundaries.
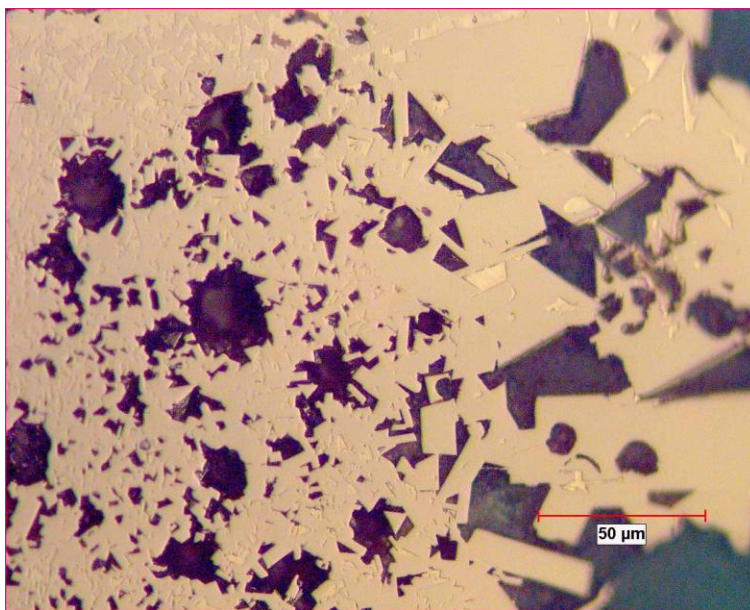
Figure 10. LSP affected tip of the tungsten carbide/cobalt rod.

These observations suggested that etching may be possible with the LSP, however the accompanying WC grain growth was an unwanted side effect that posed a serious issue when investigating diamond LSP CVD. The added kinetics of diamond nucleation on dynamic growing grains complicates the system considerably. As a result, we resolved to use a substrate with lower reactivity at high temperatures, at least initially. Tungsten and molybdenum were suitable substitutes.

3.3.2 Tungsten

1" by 1" by 1/4" tungsten plates were purchased. We ground the surfaces flat with SiC paper then polished them using a series of abrasive diamond particle suspensions. A final polish was attained using colloidal silica particle < 1 μm.

For selected experiments, the surface was seeded with diamond particles. One problem was the hardness of tungsten: could the diamond particles be mechanically pressed or wedged into the surface permanently, or should they simply lie on the surface freely? With a fully polished sample, we could easily investigate the adhesion of the diamonds using SEM.

The polished tungsten substrates were immersed in a suspension of acetone and diamond powder (particle size < 1 μm). The samples were subjected to ultrasonic agitation for a half hour, then removed. Figures 11a-11c show the results.
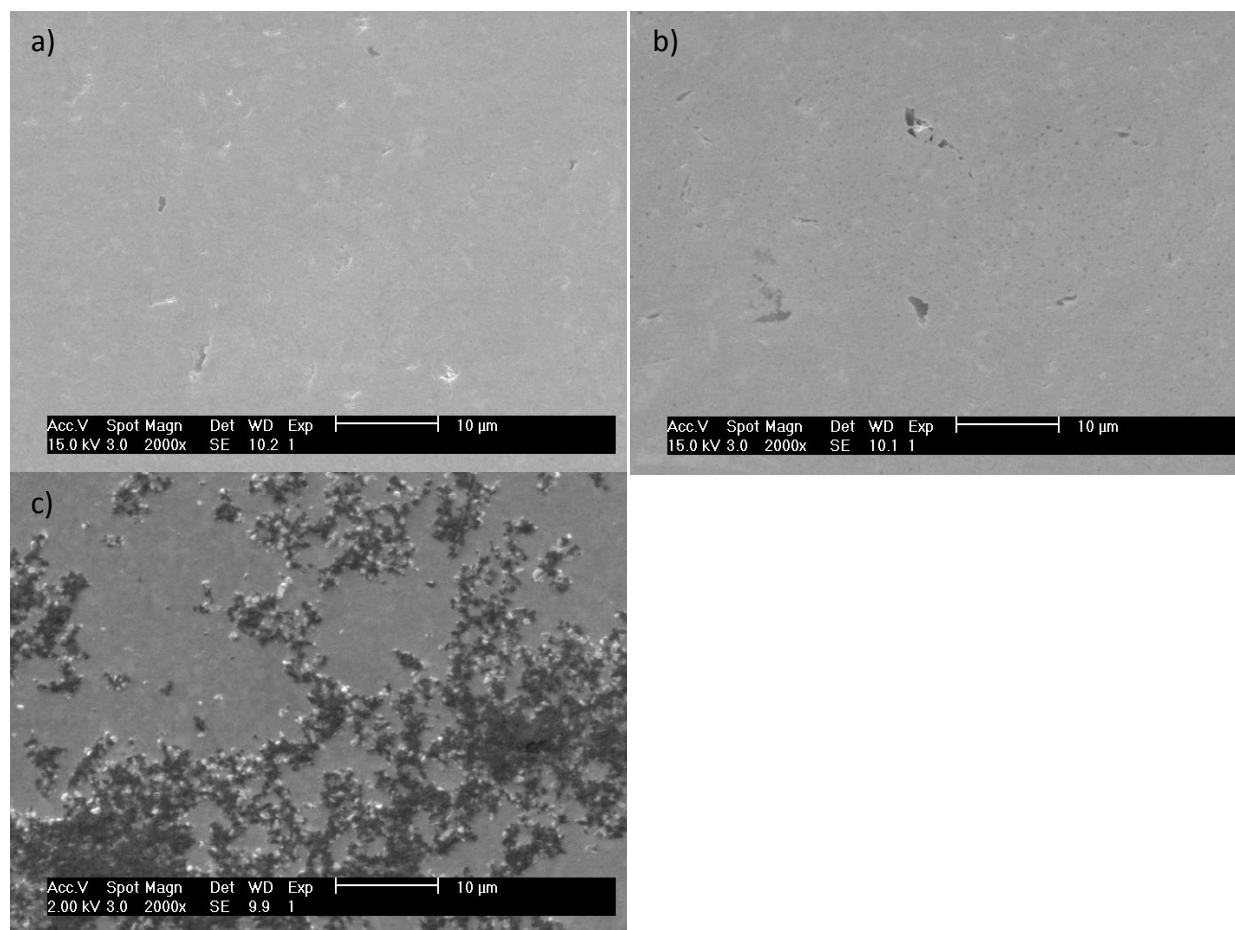
Figure 11. a) Polished tungsten without seeding. b) Polished tungsten with seeding, then cleaned with acetone. c) Polished tungsten with seeding, not cleaned with acetone

The diamond particles did not fully embed into the surface of the tungsten by ultrasonic seeding; they were washed away with acetone in figure 11b. For diamond LSP CVD, it may be simply required that the diamonds lie on the surface as nucleation sites, as in figure 11c, and that the energy of the plasma will rapidly sinter the particles in place. On the contrary, currents from the precursor gas could blow the particles away, thus removing the nucleation sites and rendering the pretreatment useless. Several experiments were developed to test these hypotheses to determine the effectiveness of diamond seeding.

4   Results and Discussion

4.1   LSP Exposure to Polished Tungsten

The first experiment determined whether the stage could adequately keep the temperature of a polished tungsten substrate below 1000°C. The experimental parameters were as follows: the laser power was 3 kW, precursor gas flow rate was 9 L/min, off-focal distance was an arbitrarily assigned 21.425 mm, and the cooling stage water flow was maximum. The off-focal distance was larger than anticipated for LSP CVD experiments in order to reduce substrate heating in this initial test.

A plasma was successfully ignited and exposed to the substrate for 300 s, tracking the temperature using the thermocouple. Figure 12 shows the temperature profile for this experiment.
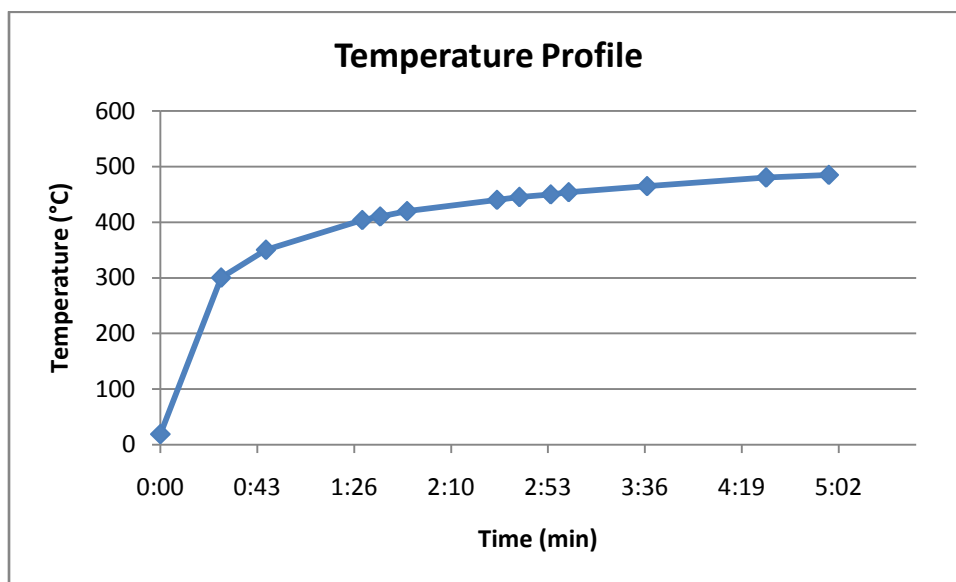

Figure 12. Temperature profile: 3 kW, 9L/min, 21.425 mm off-focal distance, 300 s exposure, unseeded

It was observed that the laser nozzle was slightly warped/damaged during this test, due to the high reflectivity of the polished tungsten reflecting the laser radiation back toward the nozzle. Although the nozzle was water cooled, it still overheated.

An infrared pyrometer tracked the laser nozzle temperature during the next trial. We repeated the experiment under the same operating conditions except for a reduction in the off-focal distance to 10 mm. At this distance, species in the LSP could reach the substrate surface potentially to form a coating. The LSP was exposed to the substrate for 69 seconds before we determined that the nozzle was indeed overheating based on the pyrometer. The substrate temperature reached 650°C in this short time period; it heated faster than in the previous trial.

Two conclusions were made here. First, a lower off-focal distance resulted in greater heating of the substrate. This was due to the ionized species in the plasma colliding with the sample more frequently, imparting their energy and raising the overall kinetic energy of the surface (i.e. temperature). Secondly, the substrate reflected too much radiation and was damaging the laser nozzle. It was necessary to reduce reflectivity, increase absorbtivity, or redirect/scatter the radiation away from the nozzle. The easiest way to do this was by abrading the surface with SiC grit. A roughened surface will scatter laser irradiation, so that the majority is not reflected directly back toward the nozzle.

4.2   LSP Exposure to Abraded Tungsten with Increased Gas Flow Rate

The tungsten substrate was abraded with 600 grit SiC paper. Furthermore, the warped laser nozzle was replaced with a ceramic one to withstand higher temperatures. The precursor gas flow rate was increased to 20 L/min to reduce sample heating, the off-focal distance was 8 mm, and the laser power was 3 kW.

An experiment was planned to run for 300 s or until the thermocouple meter read 1000°C, whichever arrived first. The experiment actually ran for 46 seconds before the substrate reached its critical temperature, as shown in figure 13.
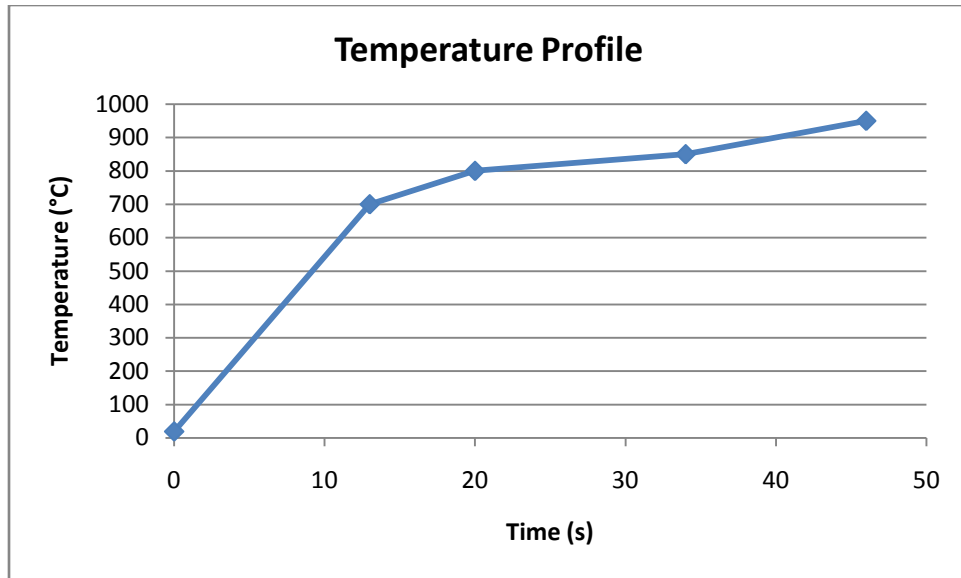
Figure 13. Temperature profile: 3 kW, 20L/min, 8 mm off-focal distance, 46 s exposure, unseeded

Since the off-focal distance was reduced by 2 mm in this trial, the heating rate increased compared to the previous experiment. Abrading the surface also increased absorption by the tungsten, contributing to increased substrate heating.

An interesting annular ring formed around the spot where the laser beam contacted the surface. Furthermore, the surface exhibited a rainbow sheen, which Schwartz et al. [4] indicated could be a sign of nanocrystalline diamond growth. This ring was investigated in the SEM using energy dispersive x-ray spectroscopy (EDS). Figure 14 shows a SEM micrograph of the ring. Three regions of interest were studied: inside the ring, outside the ring, and directly on the annular ring surface.
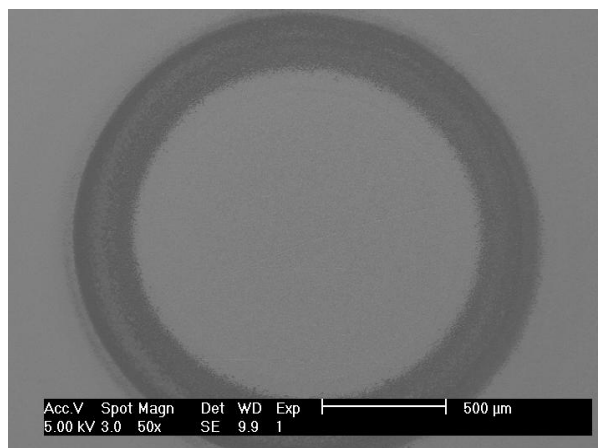
Figure 14. SEM of the annular ring: 3 kW, 20 L/min, 8 mm off-focal distance, 46 s exposure, unseeded.

EDS was performed on all three locations of the sample, starting at the center and moving outwards at 1 mm increments to new, interesting surface morphologies. On the ring, there was a strong carbon peak in the EDS spectrum, as shown in figure 15. Elsewhere on the substrate (including both inside the ring and outside), the results showed strong peaks for tungsten and oxygen. This suggested that tungsten oxide had formed on the surface.
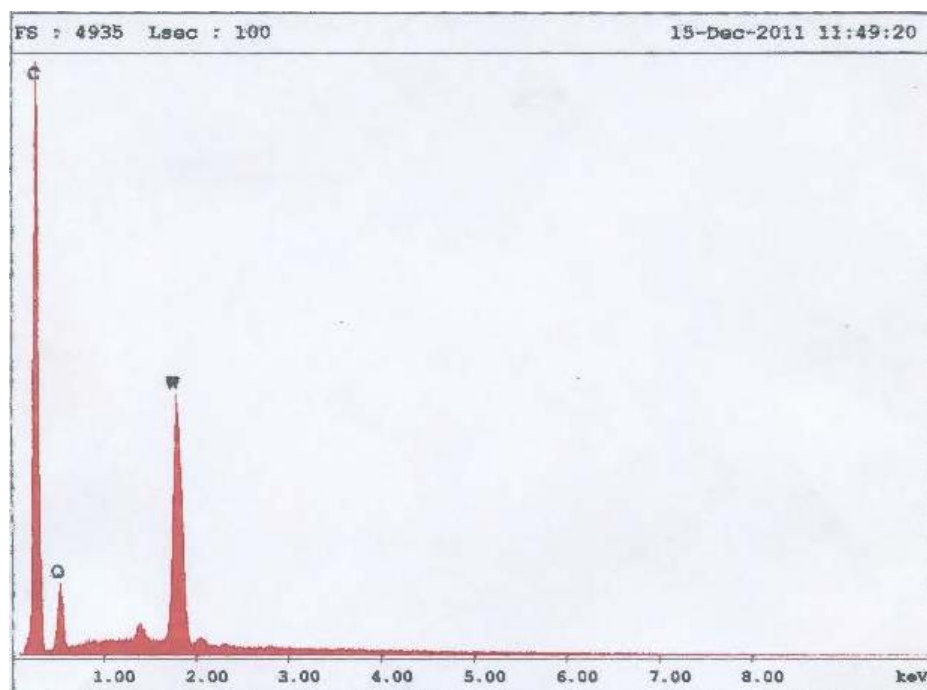

Figure 15. EDS spectrum on the annular ring

The strong carbon peak on the annular ring was investigated using Raman spectroscopy to give insights into the bonding state of this deposited film. A 488 nm laser was used for the excitation source. Figure 16a shows an SEM micrograph of the annular ring surface, with its corresponding Raman spectrum in figure 16b.
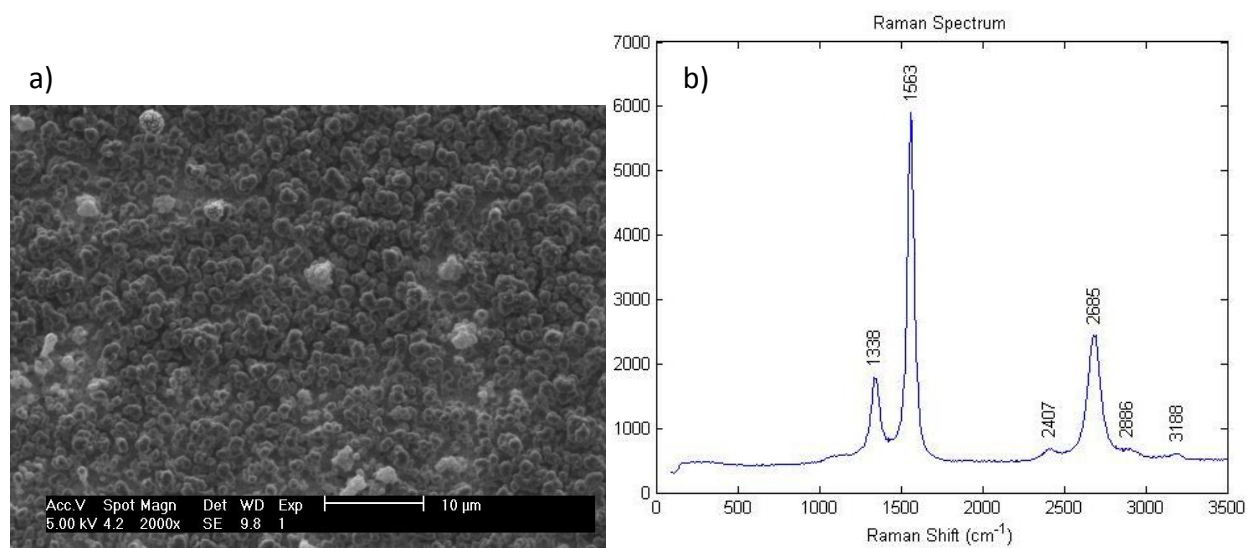

Figure 16. a) SEM micrograph of annular ring surface: 3 kW, 20L/min, 8 mm off focal distance, 46 s exposure, unseeded. b) Corresponding Raman spectrum

There was a sharp G-line peak at 1563 cm^{-1} with a broader D-line peak at 1338 cm^{-1}. Second order peaks occurred at 2407, 2685, 2886, and 3188 cm^{-1}. This spectrum matched the shape of polycrystalline graphite extremely well, but the peak positions differed from those expected for graphite. The G-line peak for graphite is around 1580 cm^{-1}. With decreasing crystallite size, this peak was expected to shift upward, not down to 1563 cm^{-1}. Furthermore, the D-line peak was lower than expected at 1338 cm^{-1}, which more closely matches diamond. This may have indicated sp3 bonding, however the sharp G-line peak suggested that sp3 bonding does not occur consistently long-range within the film. G-line peaks lower than 1575 cm^{-1} was evidence of amorphous carbon phases, but usually the D- and G-line peaks merge into a singular amorphous peak as a result of the widespread and disordered carbon bonding associated with

amorphization. In figure 16b, these two peaks are distinctly separate. One hypothesis was that

the polycrystalline graphite film experienced significant lattice distortion which caused a shift in

the primary Raman frequencies.

Figure 17a shows an area outside the annular ring with its corresponding Raman

spectrum in 17b. EDS results predicted that this zone was a tungsten oxide. The vibrational

modes of WO_3 are the W─O─W deformation mode, the W═O bending mode, and the W═O

stretching mode with corresponding Raman shifts of 276, 714, and 808 cm^{-1} [11]. Smaller second

order peaks appear around the 276 cm^{-1} shift. As can be seen in figure 17b, the peaks from the

film matched these peaks nearly perfectly (a few wavenumbers difference is not significant). It is

proven that a tungsten oxide formed on the surface.

Also of interest is the transition region from graphite to tungsten oxide in figure 18. There

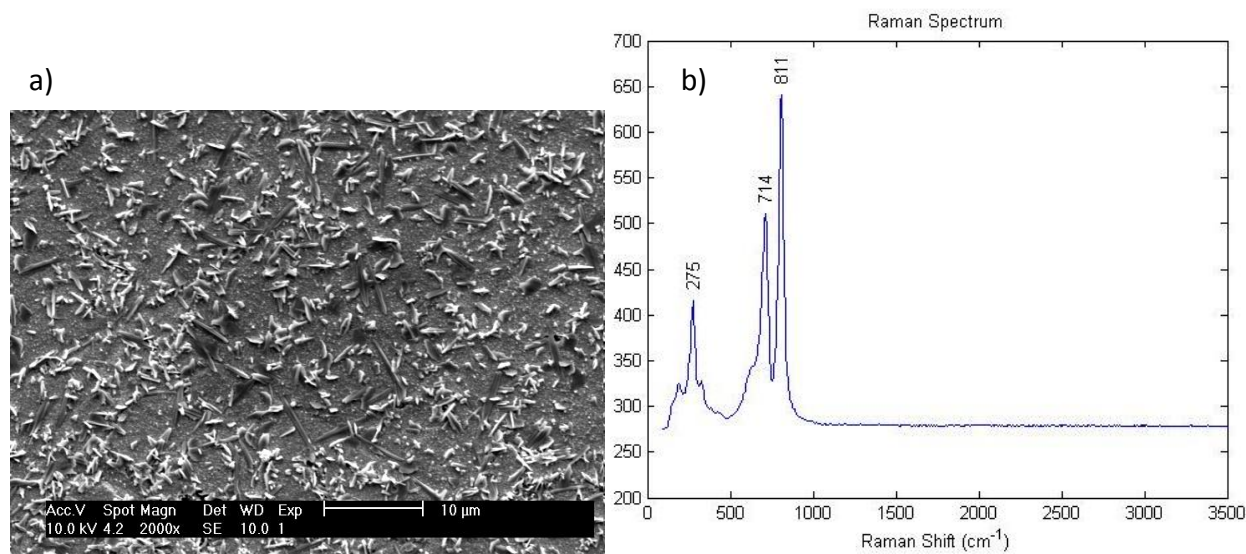was a relatively distinctive separation of these two formations on the surface.

Figure 17. a) SEM micrograph of area outside the annular ring: 3 kW, 20L/min, 8 mm off-focal distance, 46 s exposure, unseeded. b) Corresponding Raman spectrum

Although no diamond formed, it was a promising result that a form of carbon was
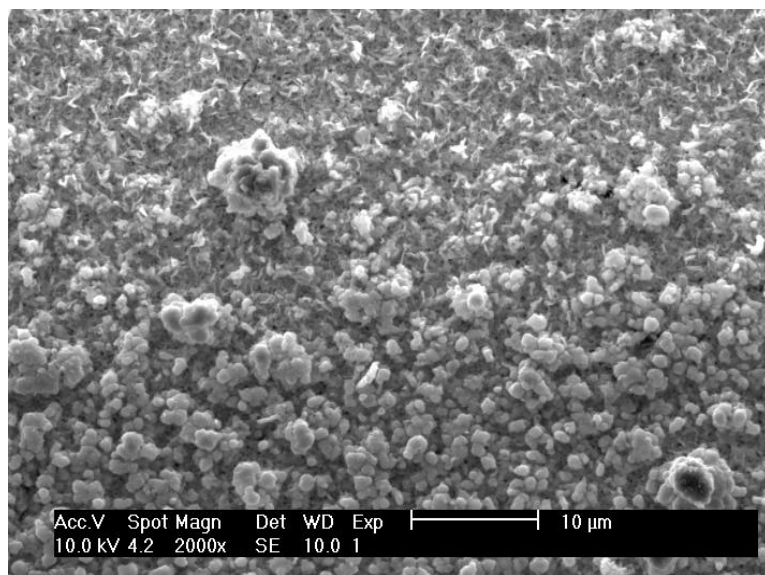
successfully deposited from the LSP.

Figure 18. Transition region between graphite ring (bottom half) and tungsten oxide (upper half).

4.3   LSP Exposure with Reduced Laser Power

A series of experiments were designed to determine why diamond did not form. One hypothesis was that the substrate temperature was too high and the cooling was insufficient. As the thermocouple read the temperature on the side of the substrate, it was not necessarily indicative of temperatures in the center, directly under the laser beam. It is possible the temperature here was well above 1200°C, the upper threshold for diamond formation. To reduce the temperature, the exposure times and laser beam power were decreased.

Two tests were performed on the same tungsten plate. The affected regions were on opposite sides of the plate along the diagonal. The first test was at a beam power of 3 kW, with a planned exposure time of 30 seconds or maximum temperature of 900°C (whichever was reached first). The gas flow rate was 20 L/min and the off-focal distance was 8 mm.

The thermocouple was closer to the plasma in this experimental setup and thus heated faster. A recorded substrate temperature of 900°C was reached in approximately 18 seconds. Figure 19 shows the temperature profile of the substrate temperature vs. time.
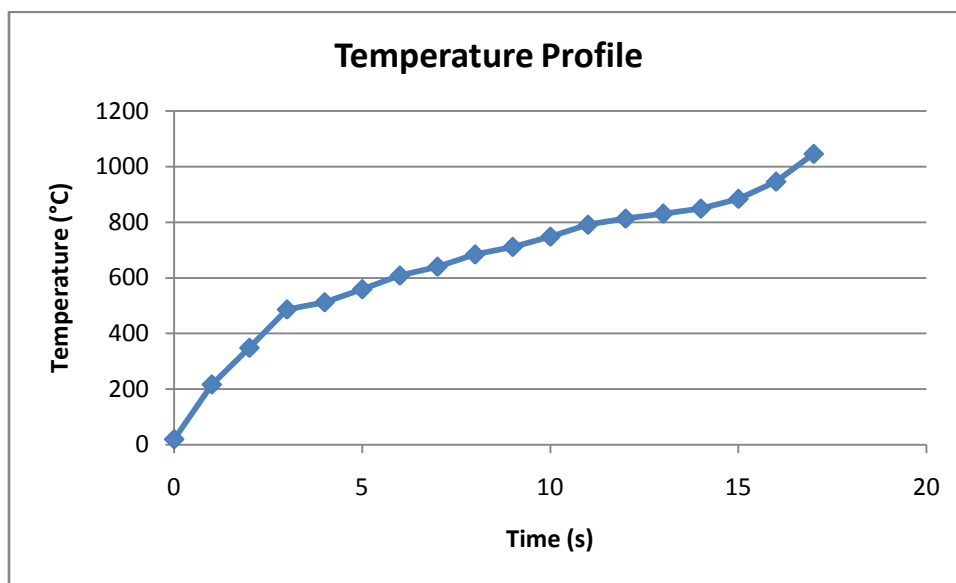

Figure 19. Temperature profile: 3 kW, 20L/min, 8 mm off focal distance, 18 s exposure time, unseeded

The temperature profile showed a rapid climb in temperature for the first 15 seconds. At the end of the test, the temperature deviated from this trend and rose at a faster rate. This might have been caused by the formation of graphite after a critical surface temperature was reached. Graphite has been shown to change the absorbtivity of the substrate, and a sudden increase in radiation absorbtion by the tungsten could explain this temperature rise at the end of LSP exposure.

An annular ring formed again, shown in figure 20. SEM and Raman spectroscopy were used to assess all three regions, as shown in figures 21-23.
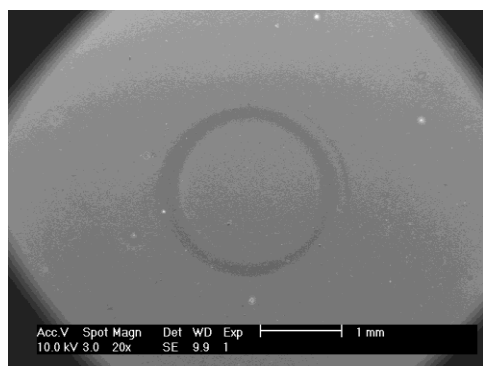
Figure 20. SEM micrograph of annular ring: 3 kW, 20L/min, 8 mm off focal distance, 18 s exposure time, unseeded
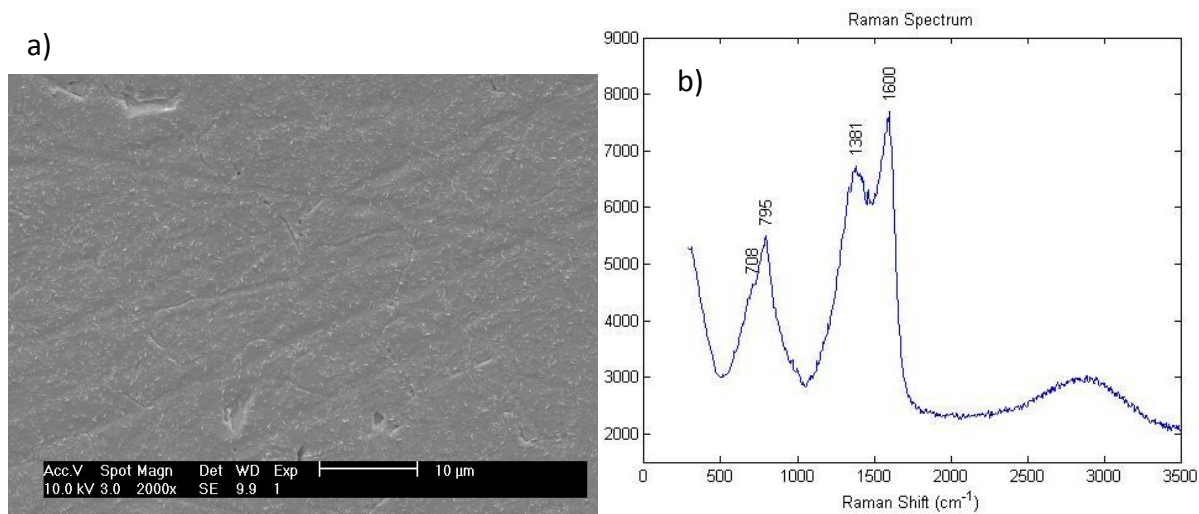

Figure 21. a) Directly under the laser beam, inside ring: 3 kW, 20L/min, 8 mm off focal distance, 18 s exposure time, unseeded. b) Corresponding Raman spectrum
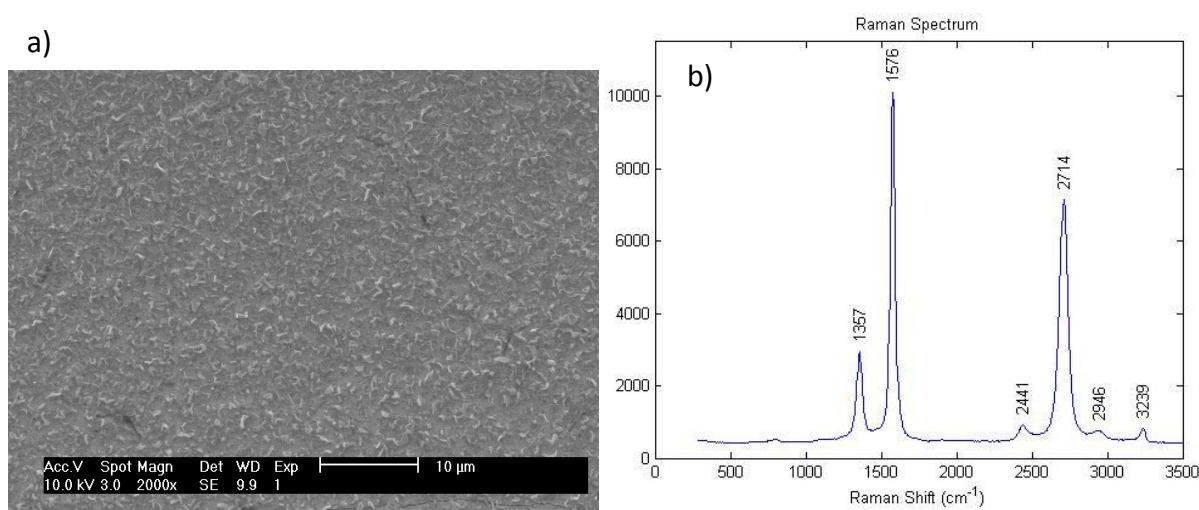

Figure 22. a) On the annular ring: 3 kW, 20L/min, 8 mm off focal distance, 18 s exposure time, unseeded. b) Corresponding Raman spectrum
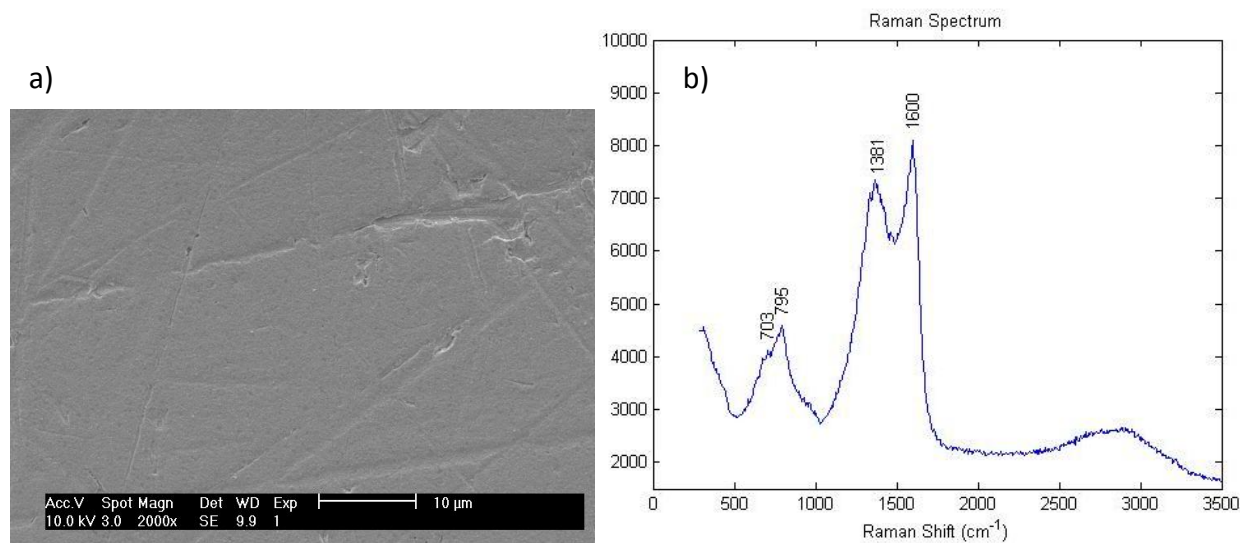
Figure 23. a) Outside the ring: 3 kW, 20L/min, 8 mm off focal distance, 18 s exposure time, unseeded. b) Corresponding Raman spectrum

The annular ring exhibited a sharp G-line peak at 1576 cm^{-1} and a D-line peak at 1357 cm^{-1}, shown in figure 22b. This was highly representative of polycrystalline graphite, unlike the shifted D- and G-line peaks from the previous experiment. Inside and outside the ring, only small particles formed on the tungsten substrate, shown in the SEM micrographs in figures 21a and 23a. The Raman spectra for each region matched one another, suggesting similar carbon phases had formed. The G-line peak shifted upward to around 1600 cm^{-1} while the D-line peak broadened. This is characteristic of polycrystalline graphite with small crystallite sizes. SEM micrographs in figures 21a and 23a supported that claim, as the particles on the tungsten surface appeared much smaller than in figure 22a directly on the annular ring. The broad peak at 2700 cm^{-1} corresponded to weak second order signals of graphite. In further analysis, these peaks were omitted since they give little information about the vibrational states present.

It was not clear what caused the asymmetric peak around 800 cm^{-1} in figures 21b and 23b. There appeared to be two peaks around 705 and 795 cm^{-1} which overlap to form a singular asymmetric one. These peaks were close to reported tungsten oxide Raman shifts, although they

are not identical in shape or position. It was hypothesized that a tungsten carbide formed on the surface instead. The W-C stretching mode exhibits a Raman shift at 800-807 cm^{-1} with a weaker shift at 685-693 cm^{-1} [12]. These bands have been shown to merge together with annealing treatments up to 800°C [12]. The peaks above still do not match these either. Lee et al. [9] recorded a symmetric broad peak around 760 cm^{-1} during their investigation of polycrystalline graphite films, which they attributed to an instrumental artifact along with scattering from nonzone-center phonons. In this experiment, the small particle size of the deposited film might account for a change in Raman band frequency due to edge phonon interactions.

For the second experiment, the unaffected sample side was abraded with 600 grit SiC paper to remove any oxides formed in the previous experiment and was cleaned with acetone. The laser power was reduced to 2 kW and the tungsten plate was again exposed to the LSP for 18 seconds. As plasma did not form with this beam power, it was increased to 2.5 kW. Figure 24 shows a temperature profile. The temperature never rose above 600°C.
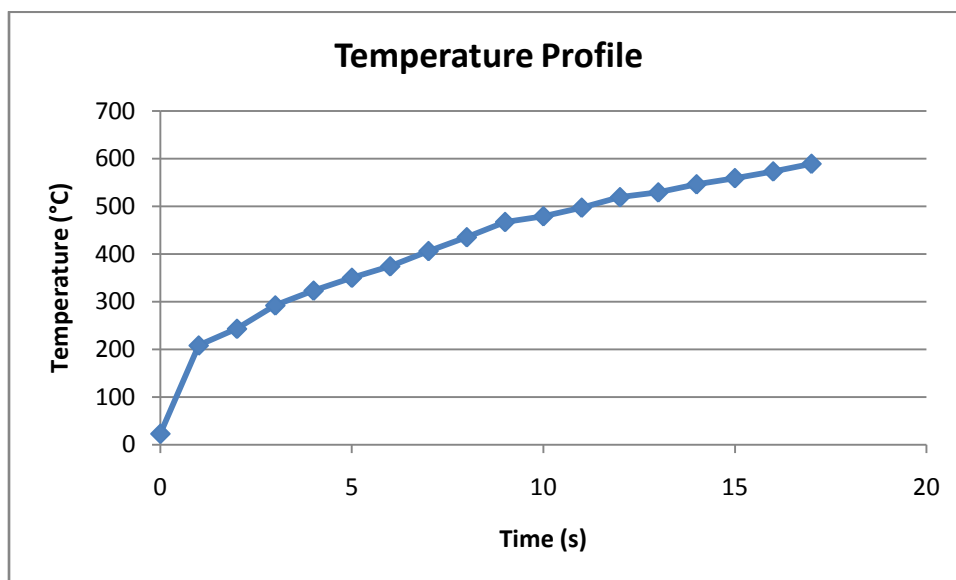

Figure 24. Temperature profile: 2.5 kW, 20L/min, 8 mm off focal distance, 18 s exposure time, unseeded

From the naked eye, no ring appeared to a have formed, although a blue spot under the path of the laser beam had formed, as shown in figure 25. The region was investigated with SEM and Raman spectroscopy.
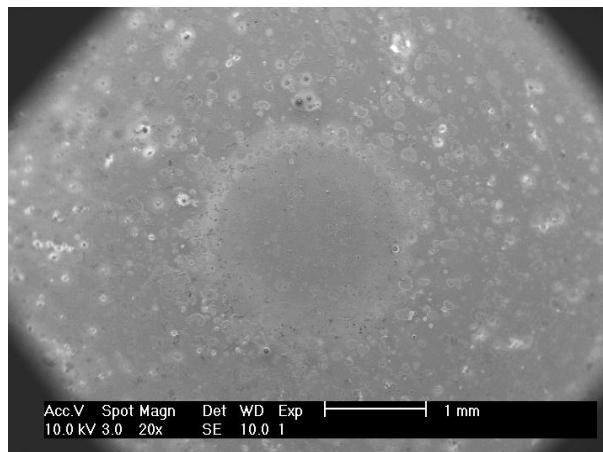

Figure 25. Affected region under laser beam, 2.5 kW methane LSP on scratched tungsten

Figure 26 shows the area directly under the laser beam with its corresponding Raman spectrum. Small artifacts indicative of that in figure 26a appeared throughout this inner region. Their exact composition is unknown. The D- and G-line peaks at 1367 and 1600 cm^{-1} in figure 23b suggest that graphite formed, although their signals were weak. An oxide likely formed, with merged peaks at 718 and 795 cm^{-1}.

Interesting spots formed on the outside surface of a circular region centered at the point of beam impact, shown in figure 27. Figure 28 shows a SEM micrograph of the boundary region between the tungsten plate and a spot. Figure 29a shows a zoomed in view of a spot, with its corresponding Raman spectrum in figure 29b. This spectrum showed the presence of graphite and a tungsten oxide, similar to the region under the laser beam with no noticeable surface formations other than the artifacts in figure 26a.

The spots were not uniformly distributed outside the central circular region and appeared haphazardly. It was unclear why a continuous annular ring did not form as it did in past

experiments. Perhaps trace tungsten oxide crystals remained on the surface from the previous experiment and experience growth when exposed to the laser beam. The fact that no strong graphite or carbon phase formed on the surface was a significant result.
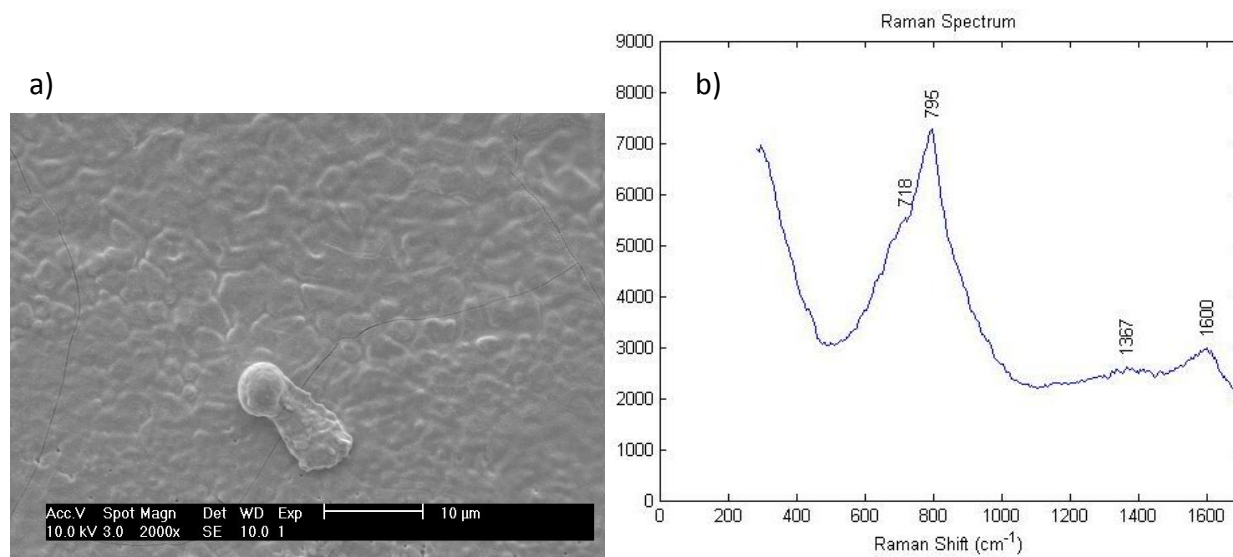

Figure 26. a) Directly under the laser beam: 2 kW, 20L/min, 8 mm off focal distance, 18 s exposure time, unseeded. b) Corresponding Raman spectrum
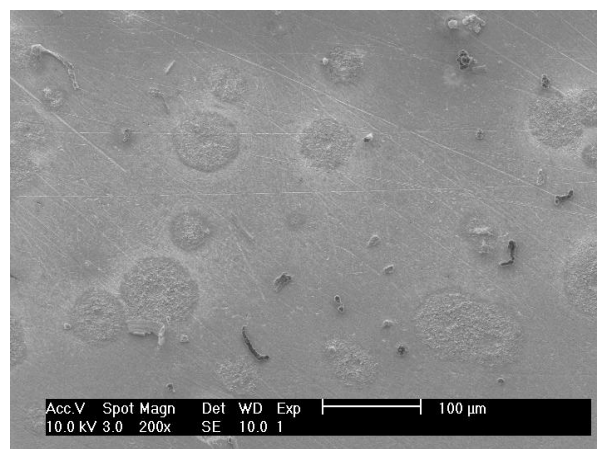

Figure 27. Isolated spots on the surface: 2 kW, 20L/min, 8 mm off focal distance, 18 s exposure time, unseeded
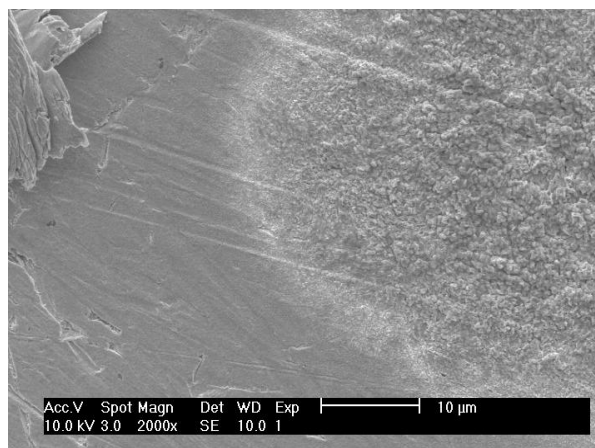
Figure 28. Boundary region between tungsten plate (left) and affected spot region (right): 2 kW, 20L/min, 8 mm off focal distance, 18 s exposure time, unseeded
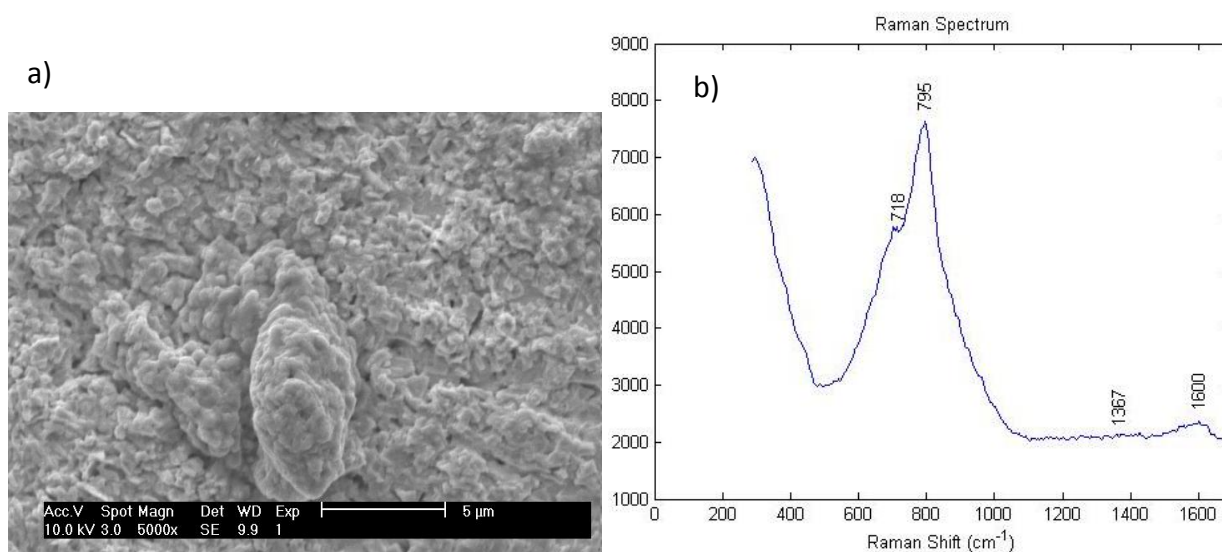
Figure 29. a) Zoomed view of spot region: 2 kW, 20L/min, 8 mm off focal distance, 18 s exposure time, unseeded. b) Corresponding Raman spectrum

4.4   LSP Exposure with Diamond Seeded Substrate

Another hypothesis as to why diamond did not form in the initial experiments was because the surface was not seeded with diamond prior to LSP exposure, as in previous work. To check, the surface of a polished tungsten plate was abraded with 600 grit SiC paper, then ultrasonically seeded in a diamond powder-acetone suspension for 30 min. All of the same

parameters were used as in the first methane LSP experiment—3 kW beam power, 20 L/min precursor gas flow rate, 8 mm off-focal distance. The only difference was that the surface was seeded with diamond. The beam was focused in the middle of the sample.

We planned to expose the sample to the LSP for 46 seconds (the same exposure time as the previous experiment) or until the substrate reached a temperature of 900°C. We were able to hold in position for 46 seconds before it reached a critical temperature. Figure 30 shows a temperature profile.

An annular ring formed just as it did the last time, shown in figure 31. This ring was investigated using SEM and Raman spectroscopy.
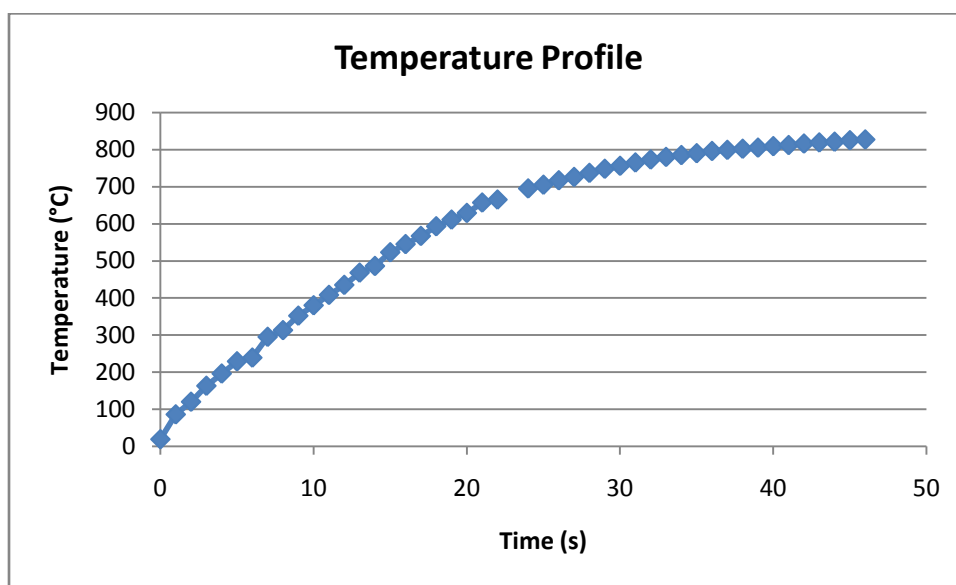

Figure 30. Temperature profile: 3 kW, 20L/min, 8 mm off focal distance, 46 s exposure time, seeded with diamonds
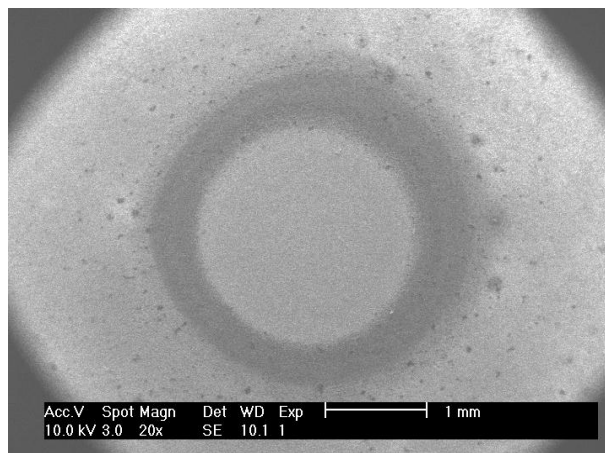
Figure 31. SEM micrograph of annular ring: 3 kW, 20L/min, 8 mm off focal distance, 46 s exposure time, seeded with diamonds

Particle growth appeared just before reaching the inner annular ring. Tiny "carrot" structures can be seen in figure 32a with a Raman spectrum recorded in the same general location in figure 32b. These formations could not be seen using the optical microscope on the confocal Raman spectrometer, so it is unclear whether the spectrum is indicative of the structures or not. They appear to be a tungsten oxide based on the peaks at 713 and 811 cm^{-1}. Moving into the
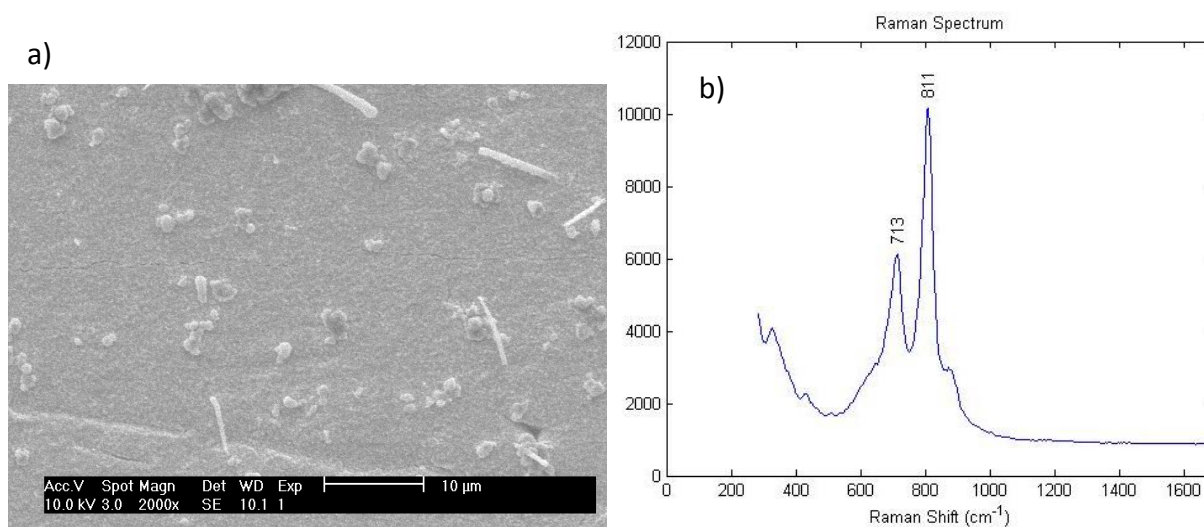

Figure 32. a) Approaching the annular ring from the inside, "carrot" structures appear: 3 kW, 20 L/min, 8 mm off focal distance, 46 s exposure time, seeded with diamonds. b) Corresponding Raman spectrum

border region of the annular ring, the "carrots" were still visible, with a darker carbon phase
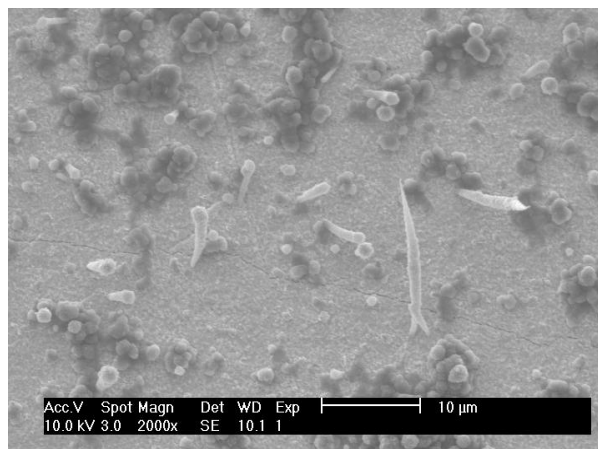
present as well, shown in figure 33.

Figure 33. "Carrot" structures appear mixed with darker carbon phases just before reaching the annular ring

The surface morphology changed across the annular ring in this experiment. On the inner

annular ring, the deposited film appeared less dense with the tungsten substrate still visible in

figure 34a. Figure 34b shows the Raman spectrum at this location and revealed the presence of

graphite. On the outer annular ring in figure 35a, the film is more dense and the tungsten is no

longer visible. The Raman spectrum in figure 35b shows that graphite and tungsten oxide had

formed. It is believed that the sharper crystallites present, magnified in figure 36, are tungsten

oxide that formed on the surface.

Also of interest were numerous black dots that had formed haphazardly on the annular

ring and on the region just outside of the ring, shown in figure 37a with its corresponding Raman

spectrum in figure 37b. Graphite was identified along with an unusual peak at 1836 cm^{-1}. This

peak did not correlate to any carbon phase, tungsten oxide, or tungsten carbide. It is unknown at

this time. A higher magnification SEM micrograph of the black spot can be seen in figure 38.

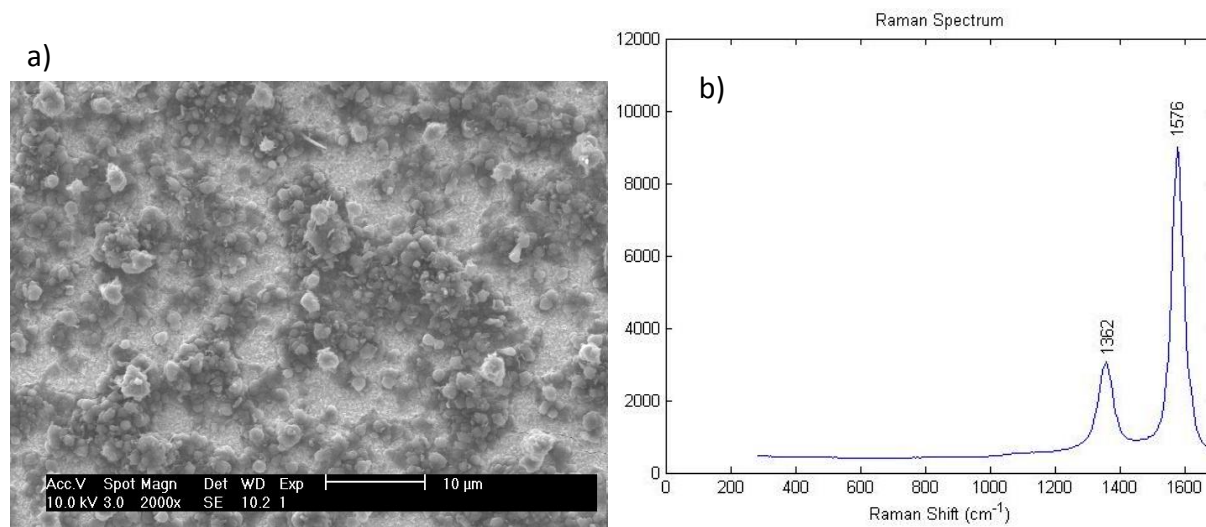Figure 34. a) On the ring, in a less dense region closer to the center. b) Corresponding Raman spectrum
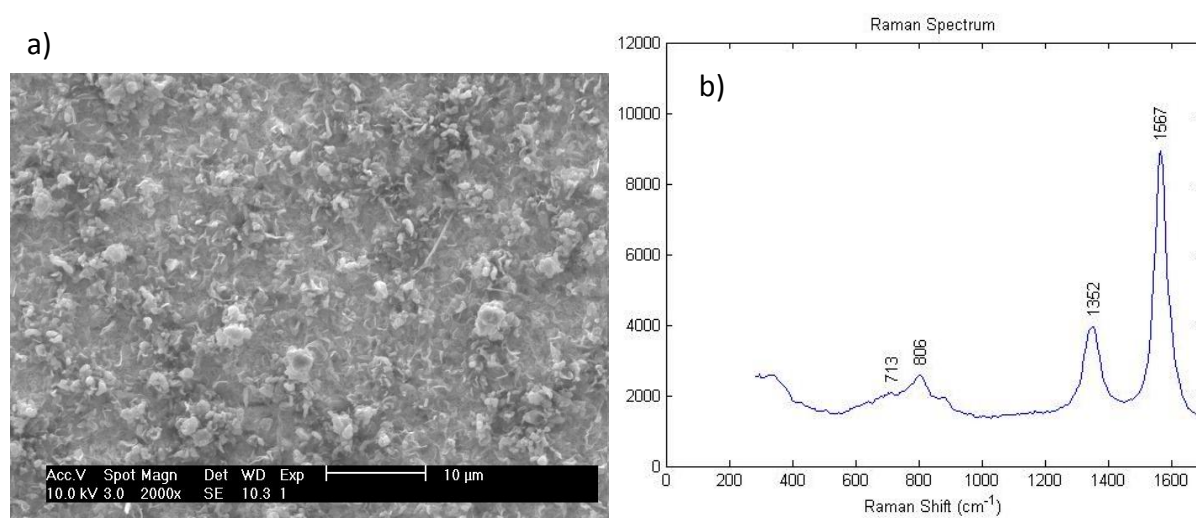

Figure 35. a) On the ring, in a more dense region closer to outward edge. b) Corresponding Raman spectrum
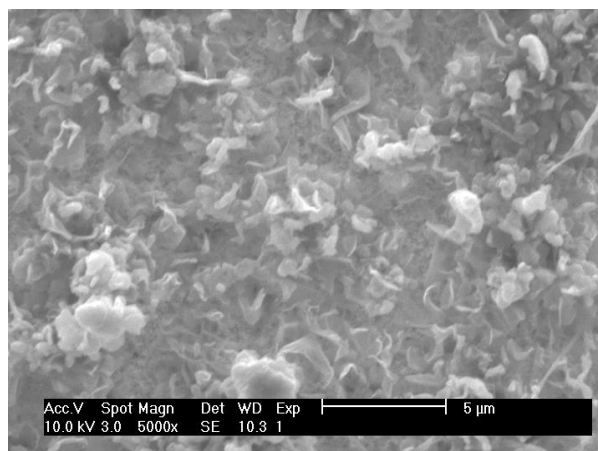
Figure 36. Figure 35a under higher magnification
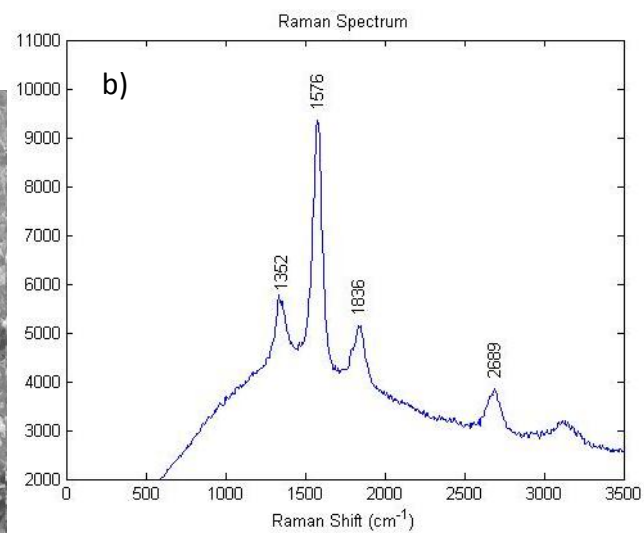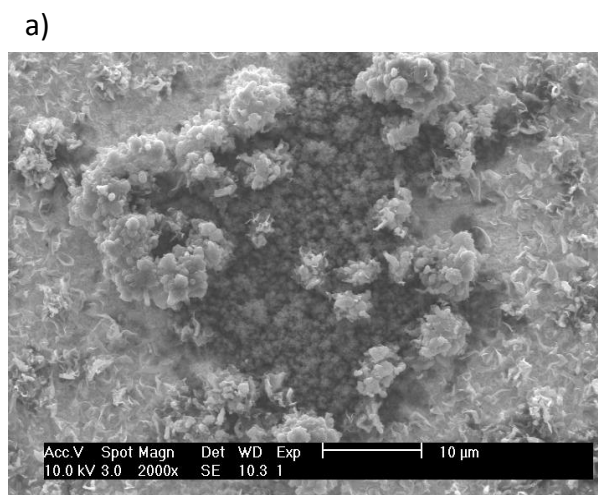
Figure 37. a) Black spot on the annular ring surface. b) Corresponding Raman spectrum
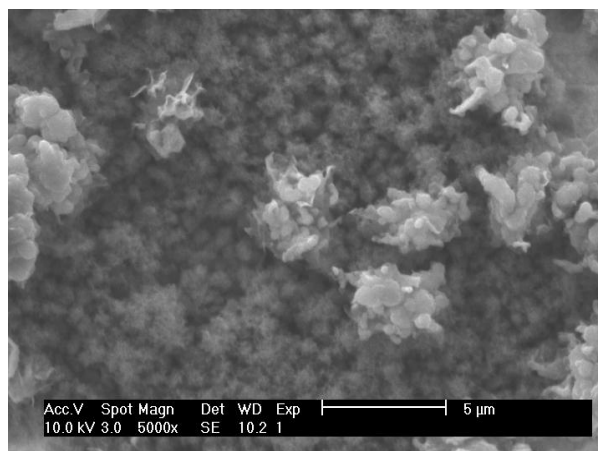
Figure 38. Figure 37a under higher magnification.

Outside the annular ring, diamond particles appeared in figure 39a. The Raman spectrum of this region in figure 39b revealed the presence of a polycrystalline diamond film with a sharp characteristic diamond peak at 1333 cm^{-1}. Figures 40a and 40b show what the surface looked like before and after LSP exposure, respectively. The diamond particles were more dense after LSP exposure than before, suggesting that the polycrystalline film grew. A technique to determine growth rate was beyond the scope of this research.
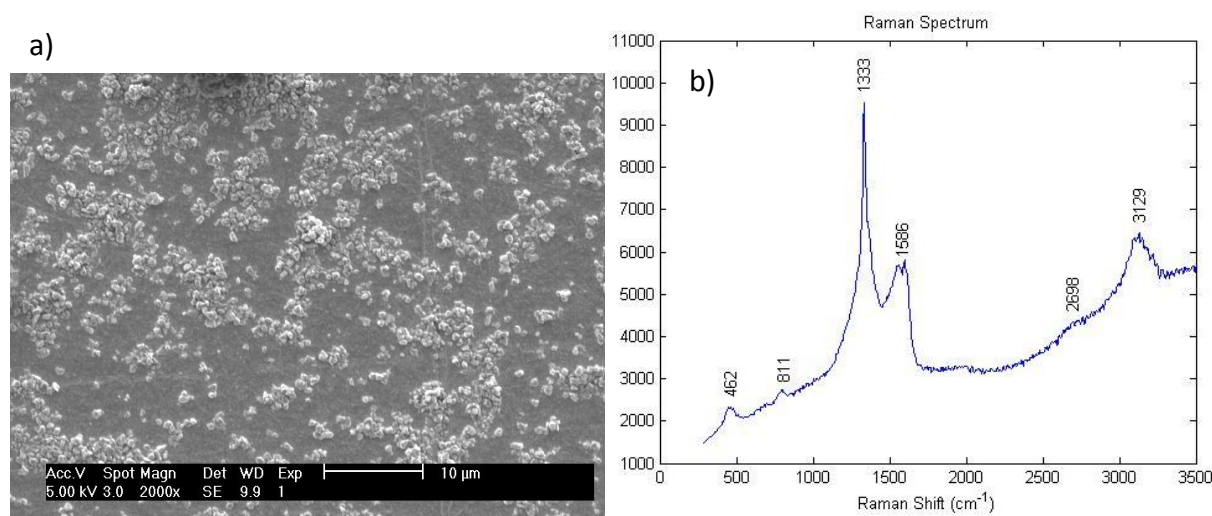
Figure 39. a) Outside of annular ring, diamond particles appear. b) Corresponding Raman spectrum
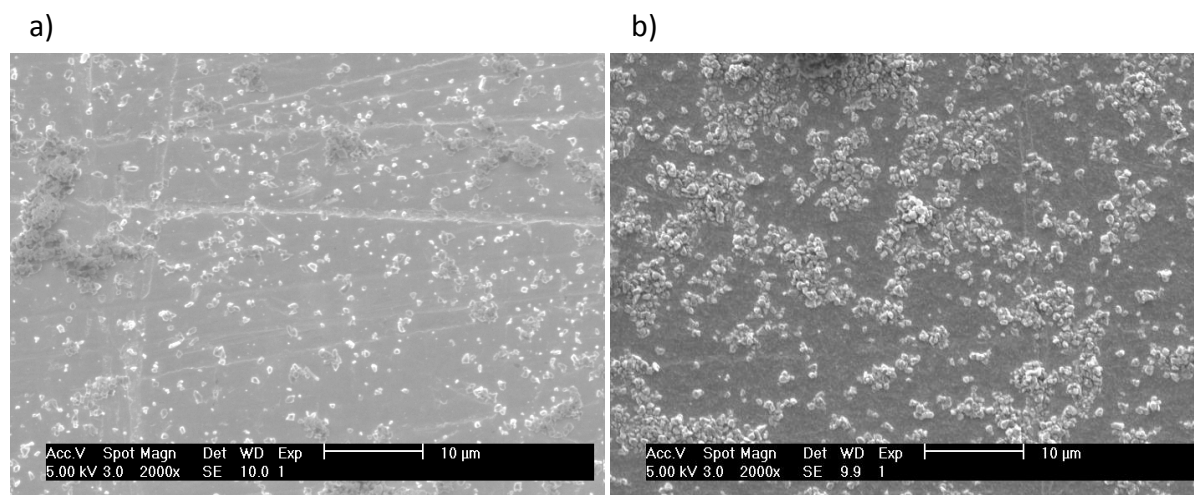
Figure 40. a) Substrate surface before LSP exposure. b) Substrate surface after LSP exposure.

Bolshakov et al. showed similar results in one of their papers [5]. Figure 41a shows a picture of their affected tungsten sample, with a distinct ring that closely matches ours in figure 41b. It should be noted that their ring contained two bright spots corresponding to the beam mode of their laser. They also show the Raman spectra of five different points on the sample in figure 41c. The spectra at location 1 has a sharp G-line peak at 1580 cm^{-1} and a weak broad D-line peak around 1360 cm^{-1}, suggesting that a polycrystalline graphite film had formed. There are no strong signals at location 2, meaning no carbon phase was deposited in that region. At location 3, the D- and G-lines are representative of graphite, but a small sharp peak at 1335 cm^{-1} suggests that sp3 bonding was present. This was the beginning area of diamond formation. At locations 4 and 5, a sharp peak at 1335 cm^{-1} with a G-line peak around 1580 cm^{-1} is indicative of a polycrystalline diamond film.

For comparison purposes, we have replicated these spectra using our Raman data at the corresponding points of interest in figure 41d. Raman data from a fifth location was not taken because the spectra and deposited film from locations 4 and 5 are virtually identical. It can be seen that the Raman spectra from this project and the work from Bolshakov et al. match each other very closely, showing that we were able to replicate their experiment. This was a promising result and the major goal of the thesis.

One major question concerns the role of the LSP. Did the carbon radicals in the plasma reach the surface to produce and grow diamond, or did the heat from the plasma graphitize the already present diamond particles on the surface? If a continuous diamond film can be grown across the surface, it can be assumed that the LSP serves as a carbon source for diamond CVD.
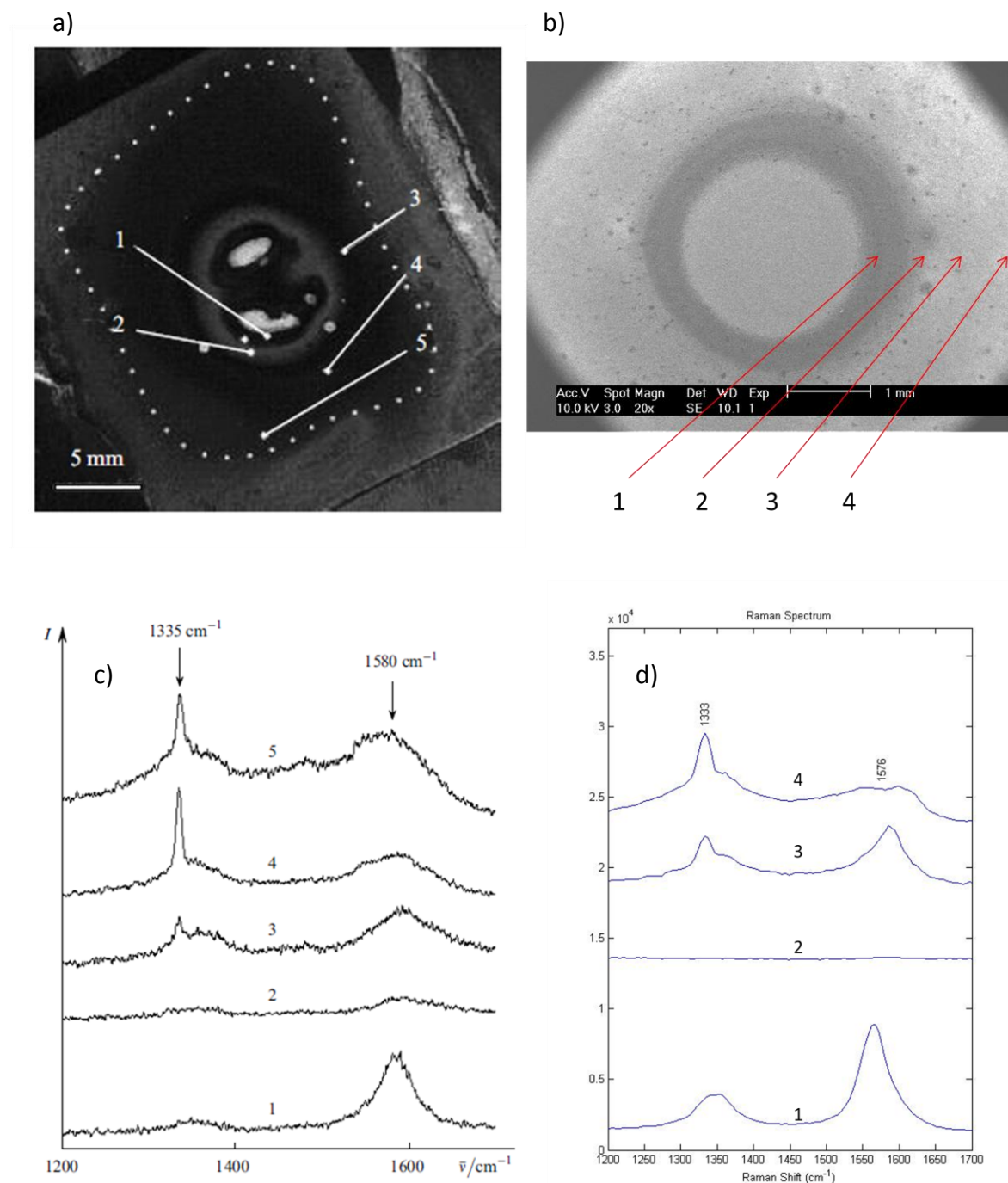
Figure 41. a) Photograph of a sample produced by Bolshakov et al., taken from [5]. The numbers correspond to areas where Raman spectra were taken. b) SEM micrograph of the annular ring from this project, with the numbers corresponding to areas where Raman spectra were taken. c) Raman spectra from Bolshakov et al. [5] d) Raman spectra from this project.

5   Conclusion

An investigation on the formation of diamond using laser sustained plasma chemical vapor deposition was conducted in this thesis. A cooling stage was first designed to maintain substrate surface temperatures below 1000°C. The experiments of Bolshakov et al. were successfully reproduced by creating polycrystalline graphite and polycrystalline diamond on the surface of tungsten. Carbon allotropes were differentiated using Raman spectroscopy, and the surface morphology was studied using optical microscopy and SEM. Tungsten oxide was identified on the surface using EDS and Raman spectroscopy.

Suggestions for Future Work

Future work will continue the investigation of diamond LSP CVD. A future goal is to form a continuous diamond film and determining the growth rate. Once accomplished, an optimization process can be developed to yield a uniform film on the substrate. Another goal is to eliminate the formation of tungsten oxide. Our research group has previously produced stoichiometric titanium nitride coatings with no oxide using a nitrogen LSP and titanium substrate. A gas containment system is not required if the plasma is scanned across the surface at a sufficiently high speed. The reactants in the plasma effectively block atmospheric gases from reaching the surface, and a reducing atmosphere is locally created to prevent oxidation. Scanning tests could possibly resolve the issue of oxidation.

Other plans include determining film growth rates, resolving the question of seeded diamond graphitization from the LSP, and altering experimental configuration to attain a reducing atmosphere.

Appendix A
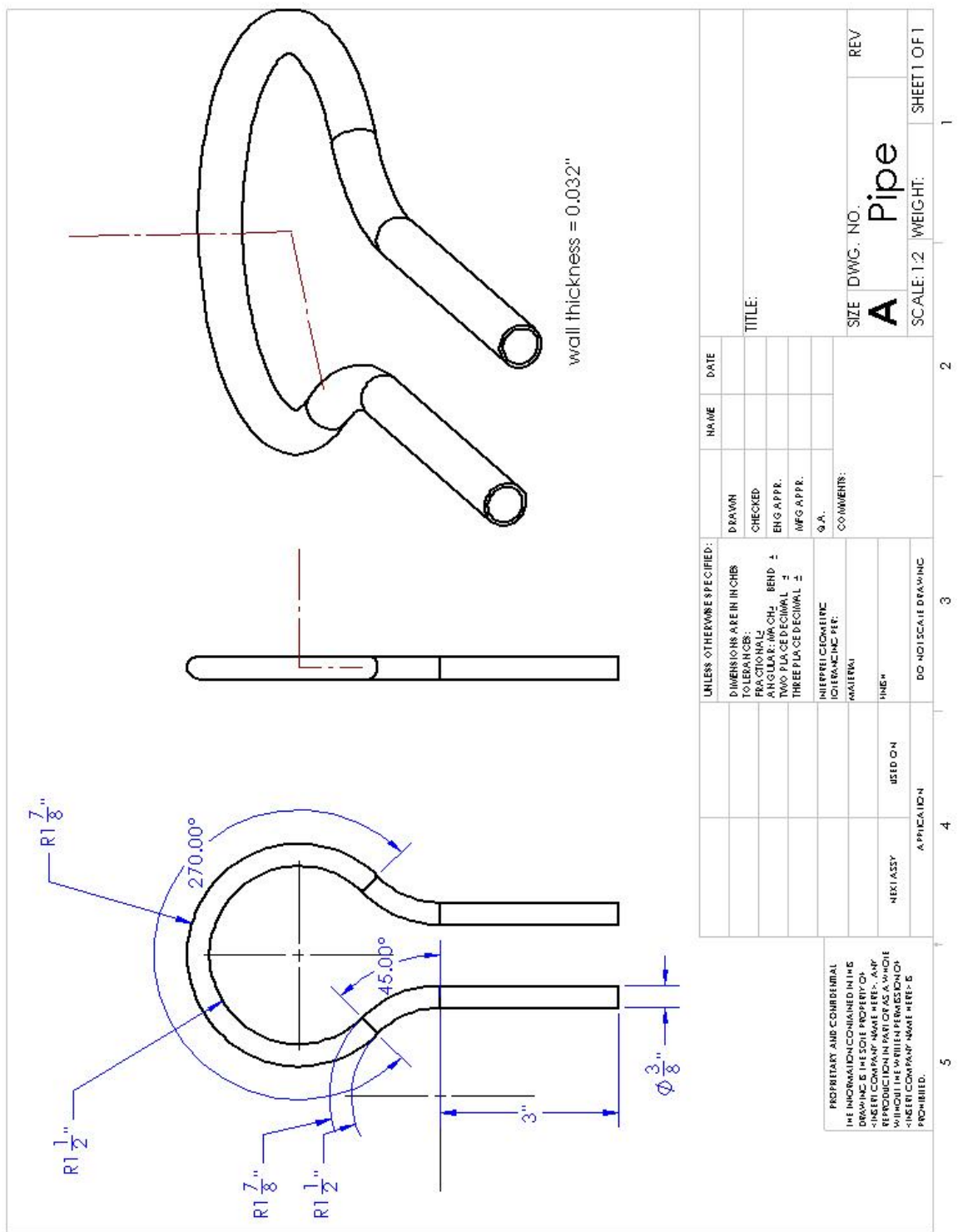
Appendix B
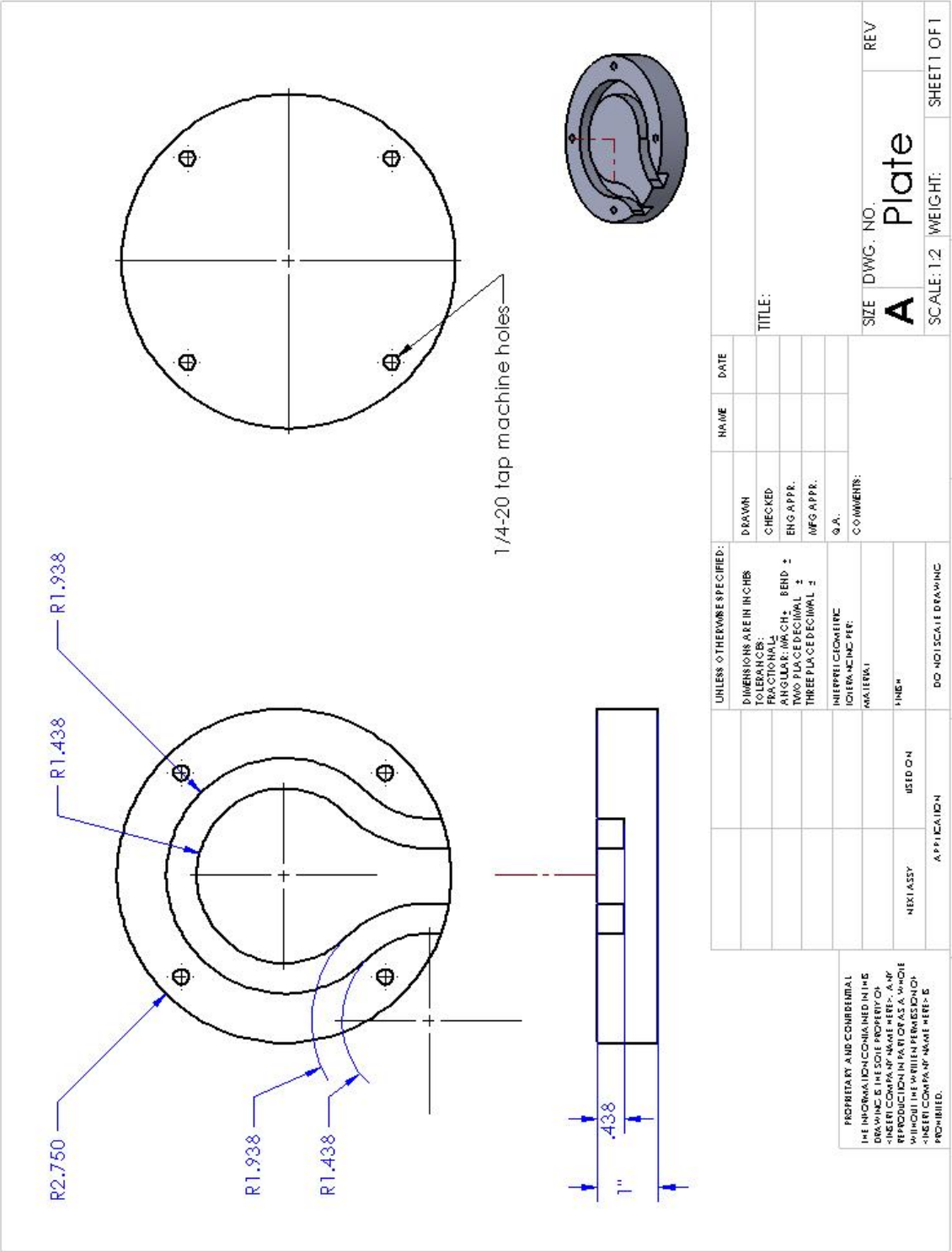
References

[1]   Liu, H. & Dandy, David. (1995). *Diamond chemical vapor deposition: Nucleation and early growth stages*. Park Ridge, New Jersey: Noyes Publications.

[2]   Bolshakov AP. Laser plasma CVD diamond reactor. *Diamond and Related Materials*. 2001;10(9-10):1559-1564. Available at: http://linkinghub.elsevier.com/retrieve/pii/S0925963501004083.

[3]   Varnin VP, Laptev Va, Ralchenko VG. The state of the art in the growth of diamond crystals and films. *Inorganic Materials*. 2006;42(S1):S1-S18. Available at: http://www.springerlink.com/index/10.1134/S0020168506130012.

[4]   Schwarz J, Meteva K, Grigat A, Schubnov A, Metev S, Vollertsen F. Synthesis of diamond coatings on tungsten carbide with photon plasmatron. *Diamond and Related Materials*. 2005;14(3-7):302-307. Available at: http://linkinghub.elsevier.com/retrieve/pii/S0925963504003656.

[5]   Bolshakov AP, Vostrikov VG, Dubrovskii VY, Konov VI, Kosyrev FK, Naumov VG, Ral'chenko VG. A laser plasmotron for chamberless deposition of diamond films. *Quantum Electronics*. 2005;35(4):385-389. Available at: http://stacks.iop.org/1063-7818/35/i=4/a=A19?key=crossref.3fc0a91192a1e7f015a4be5056e345f1.

[6]   Metev S. New technology for high rate synthesis of PC-diamond coatings in air with photon plasmatron. *Diamond and Related Materials*. 2002;11(3-6):472-477. Available at: http://linkinghub.elsevier.com/retrieve/pii/S0925963501007324.

[7]   Konov VI, Prokhorov AM, Uglov SA, Bolshakov AP, Leontiev IA, Dausinger F, Hügel H, Angstenberger B, Sepold G, Metev S. CO_2 laser-induced plasma CVD synthesis of diamond. *Applied Physics A*. 1998;66:575-578.

[8]   Hodkiewicz J. Characterizing Carbon Materials with Raman Spectroscopy. *Thermo Fisher Scientific*. 2010.

[9]   Lee EH, Hembree DM, Rao GR, Mansur LK. Raman scattering from ion-implanted diamond, graphite, and polymers. *Physical Review B*. 1993;48(21):540-550.

[10]   Park BS, Baik YJ, Lee KR, Eun KY, Kim DH. Behaviour of Co binder phase during diamond deposition on WC-Co substrate. *Diamond and Related Materials.* 1993;910-917.

[11]   Chan SS, Wachs IE, & Murrell LL. Relative Raman Cross-Sections of Tungsten Oxides: [WO_3, $Al_2(WO_4)_3$, and WO_3/Al_2O_3]. *Journal of Catalysis.* 1984;90:150-155.

[12]   Yang BO, Wang XP, Zhang HX, Wang ZB, Feng PX. Effect of substrate temperature variation on nanostructured WC films prepared using HFCVD technique. *Materials Letters.* 2007;62(10-11):1547-1550.

Local Address: **Alan S. Githens**   Permanent Address:
203 E. Fairmount Ave., Apt. 224   asg198@psu.edu   1127 Chapel Dr
State College, PA 16801   Greensburg, PA 15601
Cell: 724-972-6687   Home: 724-832-5831

EDUCATION   **Bachelor of Science in Engineering Science**
                   The Pennsylvania State University, University Park, PA
                   Schreyer Honors College
                   Graduation: May 2012

WORK   ***Undergraduate Research Assistant***   May 2010 to present
EXPERIENCE   **Center for Multi-scale Wave Material Interaction**
                   University Park, PA

- Safely operate class 4 5kW CO_2 laser to perform research
- Investigate the ignition and maintenance of laser sustained plasmas as well as their interaction with metallic substrates
- Employ various metallography techniques to prepare tungsten carbide and titanium samples for SEM analysis
- Characterize the surface morphology of experimental specimens using SEM, optical microscopy, and Raman spectroscopy

Intern, Glass Melting and Forming Engineering May 2011 to Aug 2011
Corning, Incorporated
Corning, NY

- Evaluated a commercial high-emissivity furnace crown surface treatment to improve glass melting efficiency and to lower fuel costs
- Safely performed experiments and measurements in a 1600°C test furnace
- Assembled, maintained, and operated newly acquired spectropyrometer equipment to gather emissivity and temperature data of refractory samples
- Presented conclusive results to the department and created a poster presentation for the company-wide summer intern poster session

LEADERSHIP/   UTC Ambassador, Penn State Engineering Ambassadors
ACTIVITIES   Team Leader, Rube Goldberg Competition
                   Treasurer, Society of Engineering Science
                   Student Envoy, Engineering Science and Mechanics
                   Penn State Dance MaraTHON
                   Invited Attendee, GE Student Leadership Conference

HONORS AND   Schreyer Honors College Academic Excellence Scholarship
AWARDS   Allegheny Energy Scholarship   Richard P. McNitt Scholarship

SOFTWARE   MATLAB   MS Word   MS PowerPoint
APPLICATIONS   SolidWorks 2008   MS Excel   MicroStation V8